

M.SC. ENGG. THESIS

# Automatic License Plate Detection in Hazardous Condition

by

Samiul Azam

Student Number: 0411052025

Submitted to the

Department of Computer Science and Engineering

in partial fulfilment of the requirements for the degree of  
Master of Science in Computer Science and Engineering



Department of Computer Science and Engineering

Bangladesh University of Engineering and Technology (BUET)

Dhaka 1205

October 15, 2014

*Dedicated to my loving parents and wife.*

## AUTHOR'S CONTACT

---

Samiul Azam

Lecturer

Department of Computer Science and Engineering

United International University (UIU)

E-mail: samiul@cse.uiu.ac.bd

The thesis titled “Automatic License Plate Detection in Hazardous Condition”, submitted by Samiul Azam, Student Number: **0411052025P**, Session April 2011, to the Department of Computer Science and Engineering, Bangladesh University of Engineering and Technology, has been accepted as satisfactory in partial fulfillment of the requirements for the degree of Master of Science in Computer Science and Engineering and approved as to its style and contents. The examination held on October 15, 2014.

## Board of Examiners

1. \_\_\_\_\_

Dr. Md. Monirul Islam  
Associate Professor  
Department of Computer Science and Engineering  
Bangladesh University of Engineering and Technology, Dhaka.

Chairman  
(Supervisor)

2. \_\_\_\_\_

Dr. Mohammad Mahfuzul Islam  
Head and Professor  
Department of Computer Science and Engineering  
Bangladesh University of Engineering and Technology, Dhaka.

Member  
(Ex-Officio)

3. \_\_\_\_\_

Dr. Md. Mostofa Akbar  
Professor  
Department of Computer Science and Engineering  
Bangladesh University of Engineering and Technology, Dhaka.

Member

4. \_\_\_\_\_

Dr. Mohammed Eunus Ali  
Associate Professor  
Department of Computer Science and Engineering  
Bangladesh University of Engineering and Technology, Dhaka.

Member

5. \_\_\_\_\_

Dr. Mohammad Nurul Huda  
Professor  
Department of Computer Science and Engineering  
United International University, Dhaka.

Member  
(External)

## Candidate's Declaration

This is hereby declared that the work titled “Automatic License Plate Detection in Hazardous Condition” is the outcome of research carried out by me under the supervision of Dr. Md. Monirul Islam, in the Department of Computer Science and Engineering, Bangladesh University of Engineering and Technology, Dhaka 1205. It is also declared that this thesis or any part of it has not been submitted elsewhere for the award of any degree or diploma.

---

Samiul Azam

Candidate

# Acknowledgment

I would like to express my sincere gratitude to my supervisor Dr. Md. Monirul Islam for the continuous support of my M.Sc. study and research, for his patience, motivation, enthusiasm, and immense knowledge. His guidance helped me all along this research as well as writing this thesis. He has always pointed me in the right direction when I was lost and supported me when I was on the right path. I could not have imagined having a better supervisor and mentor for my M.Sc. study.

Besides my supervisor, I would like to thank the rest of the exam committee: Prof. Dr. Mohammad Mahfuzul Islam, Prof. Dr. Md. Mostofa Akbar, Assoc. Prof. Dr. Mohammed Eunus Ali and Prof. Dr. Mohammad Nurul Huda for their encouragement, insightful comments, and hard questions.

In this regard, I remain ever grateful to my beloved parents, who always exists as sources of inspiration behind every success of mine I have ever made.

# Abstract

Automatic detection of license plate (LP) is to localize license plate region from an image without human involvement. So far a number of methods have already been introduced for automatic license plate detection (ALPD), but most of them do not consider various hazardous image conditions that exist in many real driving situations. Hazardous condition means an image can be affected by rainy or foggy weather, may have low contrast environments (such as, indoor and night), can be blurred, having other objects in the background and may have horizontally tilted LP area. All these issues create challenges in developing effective ALPD method. In this thesis, we propose a new ALPD method which can effectively detect LP area from image in hazardous conditions. In the proposed ALPD, several innovative steps are introduced for handling the inherited issues of hazardous conditions. For rain removal, a novel method is applied that uses frequency domain mask to filter rain streaks from an image. The proposed rain removal technique performs better than the existing single-image-based rain removal approach (Kang et al. 2012). A new contrast enhancement method with a statistical binarization approach is introduced in the proposed ALPD for handling low contrast indoor, night, blur and foggy images. For correcting tilted LP, a novel Radon transform based tilt correction method is applied. To filter non-LP areas, a few unique approaches are used which are based on image entropy and average horizontal counting. This new ALPD method is tested on 850 car images having different hazardous conditions and achieves satisfactory results in LP detection. We also compare the performance of the proposed ALPD method with two existing state-of-the-art methods (Wen et al. 2011 and Hasan et al. 2013). The proposed ALPD method shows best performance among them in terms of detection rate and average running time.

# Contents

<i>Dedication</i>	i
<i>Board of Examiners</i>	ii
<i>Candidate's Declaration</i>	iii
<i>Acknowledgment</i>	iv
<i>Abstract</i>	v
<i>Contents</i>	viii
<i>List of Figures</i>	xiii
<i>List of Tables</i>	xv
<b>1 Introduction</b>	<b>1</b>
1.1 Automatic License Plate Detection . . . . .	1
1.2 Applications of ALPD . . . . .	2
1.3 Background and Motivation . . . . .	4
1.4 Objectives . . . . .	4
1.5 Overview of The Proposed ALPD . . . . .	6
1.6 Scope of The Thesis . . . . .	7
1.7 Outline of The Thesis . . . . .	8
<b>2 Preliminaries and Literature Review</b>	<b>9</b>
2.1 Introduction . . . . .	9

2.2	Preliminaries . . . . .	9
2.2.1	RGB Color to Grayscale Image Conversion . . . . .	9
2.2.2	Spatial Domain Filtering . . . . .	11
2.2.3	Discrete Fourier Transform of an Image . . . . .	12
2.2.4	Entropy of an Image . . . . .	14
2.2.5	Tamura Contrast Value . . . . .	14
2.2.6	Bernsen Binarization . . . . .	15
2.2.7	Binary Perimeter Image . . . . .	16
2.2.8	Connected Components in Binary Image . . . . .	17
2.2.9	Contrast Limited Adaptive Histogram Equalization . . . . .	18
2.2.10	Morphological Erosion and Dilation . . . . .	19
2.2.11	Radon Transform of an Image . . . . .	22
2.2.12	Wiener Noise Filter . . . . .	24
2.3	Literature Review . . . . .	26
2.4	Conclusion . . . . .	34
<b>3</b>	<b>The Proposed ALPD</b>	<b>36</b>
3.1	Introduction . . . . .	36
3.2	The Proposed ALPD Method . . . . .	36
3.2.1	Grayscale conversion, noise and rain effect removal . . . . .	38
3.2.1.1	RGB Color Image to Grayscale Conversion . . . . .	39
3.2.1.2	Rain Effect Removal . . . . .	40
3.2.1.3	Non-periodic Noise Removal . . . . .	42
3.2.2	Contrast Enhancement and Binarization . . . . .	45
3.2.2.1	Tamura-CLAHE Contrast Enhancement . . . . .	45
3.2.2.2	Standard Deviation and Mean Based Binarization . . . . .	46
3.2.3	Local Counting Filter and CCC . . . . .	51
3.2.3.1	Local Counting Filter . . . . .	52
3.2.3.2	Morphological Erosion and Dilation . . . . .	52
3.2.3.3	Cropping Connected Components . . . . .	52
3.2.4	Tilt Angle Detection and Correction . . . . .	53



3.2.4.1	Bernsen Binarization and Binary Perimeter Version of Candidate LP . . . . .	54
3.2.4.2	Radon Transform Based Tilt Angle Detection and Correction . . . . .	55
3.2.5	Filtering Non-LP Regions . . . . .	56
3.2.5.1	Filtering Non-LP Regions Based on Size, Ratio and Orientation . . . . .	57
3.2.5.2	Filtering Non-LP Regions Based on Entropy . . . . .	58
3.2.5.3	Filtering Non-LP Regions Based on Average Counting . . . . .	59
3.3	Conclusion . . . . .	59
<b>4</b>	<b>Experimental Studies</b>	<b>62</b>
4.1	Introduction . . . . .	62
4.2	Image Database and Performance Measurement . . . . .	62
4.3	Experimental Analysis on the Value of <i>div</i> . . . . .	67
4.4	Experimental Analysis on the Value of <i>k</i> . . . . .	68
4.5	Experimental Analysis on Average Counting Value . . . . .	69
4.6	Experiment on Rain-affected Images . . . . .	70
4.7	Experiment on Indoor, Day, Night, Blurry and Foggy Images . . . . .	73
4.8	Performance of Horizontal Tilt Correction . . . . .	75
4.9	Comparison with Other Methods . . . . .	75
4.10	Conclusion . . . . .	80
<b>5</b>	<b>Conclusion</b>	<b>81</b>
5.1	Summary . . . . .	81
5.2	Suggestions for Future Work . . . . .	82
	<b><i>Bibliography</i></b>	<b>86</b>

# List of Figures

1.1	Basic organization of an ALPR system. . . . .	2
1.2	Pictures of real life applications of ALPR system: ALPR system in (a) traffic law enforcement, (b) automatic toll collection, and (c) parking automation. . . . .	3
1.3	Example images of vehicle (a) in rain, (b) in fog, (c) at indoor, (d) at night, (e) having blur effect, (f) having tilted LP, (g) with background objects, and (h) without hazardous condition. . . . .	5
1.4	Organization of the proposed ALPD method. . . . .	7
2.1	An example of (a) RGB color image and its (b) red (c) green and (d) blue color components after decomposition. (Image (a) from [1]) . . . . .	10
2.2	An example of 8-bit grayscale image. . . . .	11
2.3	(a) Spatial domain filtering, (b) a grayscale image, (c) image after applying local mean filter and (d) image after applying local standard-deviation filter. (Image (b) from [1]) . . . . .	12
2.4	(a) Input image and (b) the image after applying forward DFT on the input image. (Image (a) from [1]) . . . . .	13
2.5	An 8-bit grayscale image with its entropy value. (Image (a) from [1]) . .	14
2.6	Example of images having (a) moderate contrast, (b) low contrast at dark condition and (c) low contrast at bright condition. (Image (a) from [1])	15
2.7	(a) An input image and (b) the image after applying Bernsen binarization on the input image. (Image (a) from [1]) . . . . .	16
2.8	(a) Horizontal and (b) vertical filters that are applied on binary image to get the binary perimeter version. . . . .	17

2.9	An example (a) binary image and its (b) binary perimeter version. . . .	18
2.10	An example binary image that contains 10 connected components. . . .	18
2.11	Examples of images having (a) low contrast at bright condition, (b) low contrast at dark condition and (c) high contrast. Individual histogram is placed at the right side of each image. . . . .	20
2.12	Example of (a) low contrast image, (b) resulted image after applying GHE and (c) resulted image after applying CLAHE. Individual histogram is placed at the right side of each image.(Image (a) from [2]) . . . . .	21
2.13	(a) Structuring element that is applied on the (b) input binary image. After erosion, several thin lines are removed from (c) the resulted image. (Image (b) from [2]) . . . . .	22
2.14	(a) The input binary image and (b) the resulted binary image after dilation. Same structuring element of Figure 2.13(a) is used for 3 times to increase the thickness. (Image (a) from [2]) . . . . .	23
2.15	Projection of a binary image on +45 degree and -30 degree projection line.	23
2.16	(a) A binary image where the white component have 45 degree orientation and (b) the bright spot located at 45 <sup>th</sup> column of the Radon tranformed image. . . . .	24
2.17	(a) A noise induced grayscale image, and the images after using (b) Gaussian noise filter, (c) median filter and (d) Wiener noise filter. . . . .	25
2.18	Example of (a) an input grayscale image, (b) it's edge image. The white vertical line in the edge image is the axis of symmetry which intersects the LP region of the image. . . . .	30
2.19	Example of edge image with vertical axis of symmetry. The red marked box contains the detected LP region. Small circles on the box are the points found during LP search on vertical axis of symmetry. . . . .	31
2.20	(a) An example LP region affected by shadow, (b) after applying Gaussian smoothing filter, (c) output of traditional Bernsen and (d) output of improved Bernsen. . . . .	32
3.1	Sequential stages of the proposed ALPD method. . . . .	37

3.2	Conversion from (a) RGB color image to (b) grayscale image (G1). . . .	39
3.3	Example of (a) rain affected grayscale image (G1), (b) its Fourier image (F1) and (c) the thresholded Fourier image (F2). . . . .	40
3.4	(a) The direction image, (b) an example of right half of the thresholded Fourier image (F2) and (c) the energy histogram for each direction. . . .	41
3.5	Example of (a) mask image, (b) an input rain affected grayscale image (G1) and (c) the rain removed image (G1') after applying the mask. . . .	42
3.6	Example images (a) before and (b) after applying Wiener filter. . . . .	43
3.7	Example LP images showing the effect of using Wiener noise filter in the issue of extra boundary region. . . . .	44
3.8	Example LP images showing the effect of using Wiener noise filter in the issue of Bernsen binarization. . . . .	44
3.9	Example car images showing the effect of using Tamura-CLAHE contrast enhancement. The top image is in day-light condition, the middle one is in indoor condition and the bottom image contains blur effects. . . . .	47
3.10	Performance of Tamura-CLAHE contrast enhancement over fog affected car images. . . . .	48
3.11	Examples of (a) mean image (M), (b) standard deviation image (SD) and (c) binary image (B1). . . . .	49
3.12	Artificially created images and their binarized version after applying the statistical binarization method. . . . .	50
3.13	Contrast enhanced images (G2) and their binary images (B1) after applying the second stage. The top image is affected by fog, the middle one has low illuminated night effect and the bottom image contains blur effect. . . . .	51
3.14	Example of (a) binary image (B1), (b) filtered binary image (B2) and (c) dialated binary image (B3). . . . .	53
3.15	Example of (a) dialated binary image (B3) with labeled components and (b) cropped candidate LP regions from contrast enhanced image (G3). . . . .	54
3.16	Example images of candidate LPs with their Bernsen binarized and binary perimeter version. . . . .	55

3.17	Images showing steps of tilt detection and the output candidate LP regions after tilt correction. . . . .	56
3.18	Examples of candidate LP images that are rejected as non-LP due to undersized resolution. . . . .	57
3.19	Examples of candidate LP images that are rejected as non-LP due to unsatisfied width-height ratio. . . . .	58
3.20	Examples of candidate LP images that are rejected as non-LP due to unconvinced orientation angle. . . . .	58
3.21	Examples of candidate LP images and the output images after applying vertical counting filter. Entropy based filtering decisions are also reflected at the rightmost column of the Figure. . . . .	60
3.22	Examples of candidate LP images that are rejected after applying average horizontal counting. Filtering decisions are also reflected at the rightmost column of the Figure. . . . .	61
4.1	Examples of rain affected car images from the Bangla LP database [3]. Heavy-rain affected images with (a) -30 degree rain orientation and (b) -15 rain orientation. Moderate rain-affected images with (c) -30 degree rain orientation and (d) -15 rain orientation. Light rain-affected images with (e) -30 degree rain orientation and (f) -15 rain orientation. . . . .	64
4.2	Examples of non-rain car images from the Bangla LP database [3]. (a) blurry, (b) foggy, (c) indoor (d) night and (e) day-light conditions. . . .	65
4.3	Examples of car images from the English LP database [4]. (a) left tilted, (b) straight LP, (c) right tilted and (d) night conditions. . . . .	66
4.4	Rain-removed versions (a)-(f) after applying the proposed rain removal technique on the images of Figure 4.1(a)-(f). Detected LP regions (by the proposed ALPD) are also given just below the individual image. . .	71
4.5	Example of (a) a simple non-rain car image, and it's (b) rain-affected version. (c) The rain-removed version after applying the technique [5] and (d) the rain-removed version after applying the proposed rain removal technique. . . . .	72

4.6	Example car images from Bangla LP database [3]. (a) Blur, (b) fog, (c) indoor and (d) night. Detected LP region (by the proposed ALPD) is given just below the individual image. . . . .	74
4.7	Examples of detected LP image before tilt correction, as well as, after applying proposed Radon transform-based tilt correction. Automatically detected horizontal tilt angles are also given in the middle column of the Figure. . . . .	77
4.8	Example car images from English LP database [4]. Here the top image has no hazardous condition, middle image has horizontally tilted LP and the bottom image has low contrast night condition. Also the detected LP regions by different ALPD methods are given. . . . .	78
4.9	Example car images from Bangla LP database [3]. Here the top image has no hazardous conditions, middle image has horizontally tilted LP and the bottom image has rain effects. Also the detected LP regions by different ALPD methods are given. . . . .	79

# List of Tables

2.1	Consideration level of four hazardous conditions in different state-of-the-art ALPD methods. . . . .	34
4.1	Summary of the rain-affected car image dataset (total 225 images). . . .	63
4.2	Summary of the non-rain image dataset (300 car images having normal and hazardous conditions). . . . .	63
4.3	Performance of the proposed ALPD for different values of <i>div</i> . . . . .	67
4.4	Performance of the proposed ALPD for day-light car images at different values of <i>k</i> . . . . .	68
4.5	Performance of the proposed ALPD for indoor car images at different values of <i>k</i> . . . . .	69
4.6	Performance of the proposed ALPD for foggy car images at different values of <i>k</i> . . . . .	69
4.7	Performance of the proposed ALPD for blurry car images at different values of <i>k</i> . . . . .	69
4.8	Performance of the proposed ALPD for night's car images at different values of <i>k</i> . . . . .	69
4.9	Number of misselections for different threshold values of average counting.	70
4.10	Performance of the proposed ALPD on rain-affected car images (the rain removal technique is applied beforehand). . . . .	73
4.11	Performance of the proposed ALPD on 300 non-rain car images having normal (day-light) and hazardous conditions (fog, blur, indoor and night).	75
4.12	Performance of the ALPD techniques [6], [7] and the proposed one on English car image database [4]. . . . .	80

4.13 Performance of the ALPD techniques [6], [7] and the proposed one on Bangla car image database [3]. . . . .	80
--	----



# Chapter 1

## Introduction

### 1.1 Automatic License Plate Detection

Automatic License Plate Detection (ALPD) means extracting vehicle's license plate (LP) area from an image without human intervention. It is one of the important stages of Automatic License Plate Recognition (ALPR) System [8]. In an ALPR system, there are three major stages such as,

1. Acquisition of car image by image capturing device,
2. Detection of potential LP area from the image, and
3. Feature extraction and recognition of characters.

Figure 1.1 shows the basic organization of an ALPR system. In this system, the crucial stage is the detection stage where the input is the acquired car image and the output is the portion of the image containing the potential LP [9]. Unsuccessful detection of LP will make difficult, even impossible for the next recognition stage to extract LP information. But for successful detection of LP, the detection stage needs to handle some significant issues such as,

1. LP location can be anywhere in the image,
2. There can be one or many LPs in the image,
3. LPs may have different size in the image due to camera distance,

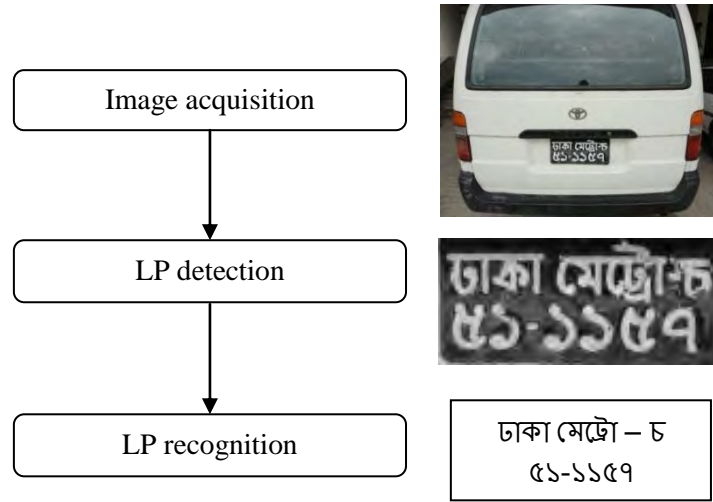


Figure 1.1: Basic organization of an ALPR system.

4. LPs may have various character and background colors,
5. An LP can be horizontally tilted due to camera position,
6. Acquired image can have poor lighting and low contrast,
7. Background of the acquired image may contains other objects similar to LP, and
8. Presence of weather effect in the acquired image.

All these issues make the ALPD a challenging research topic in the field of image processing.

## 1.2 Applications of ALPD

ALPD is an essential part of any ALPR system. The objective of an ALPR system is automatic identification of a vehicle by reading LP data from image. In an ALPR system, stationary cameras are mounted on road signs, street lights, buildings or highway overpass for capturing images of moving or parked vehicles. Then the captured images will go through a software system that will first detect possible LP location in the image, and then convert the LP data into a computer readable format using optical character

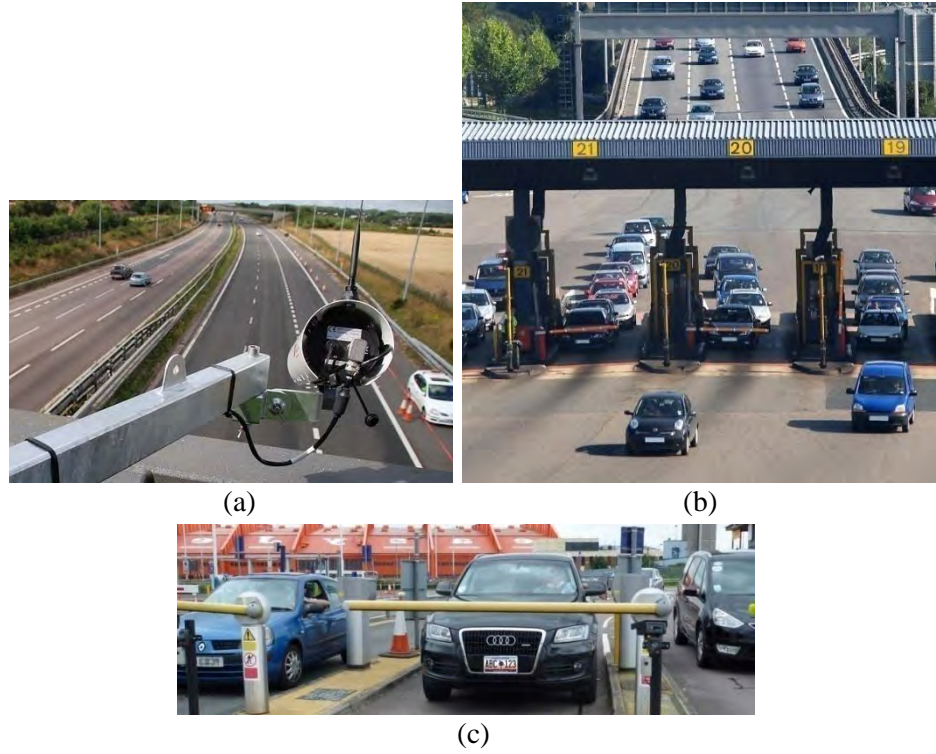


Figure 1.2: Pictures of real life applications of ALPR system: ALPR system in (a) traffic law enforcement, (b) automatic toll collection, and (c) parking automation.

recognition (OCR). The recovered identity of the vehicle can be used in real time or stored in the database for future use.

ALPD is the most non-trivial part of an ALPR system which has numerous number of real life applications. One of the important applications of ALPR system is traffic law enforcement. An ALPR system can be used for automatic and faster identification of stolen vehicles, criminal cars, speeders and traffic law breakers [10]. Even, traffic pattern analysis during peak and off-peak hours can be possible using ALPR system. Another popular application of ALPR system is automatic toll collection for highways, flyovers and bridges. This automatic approach saves time and reduces traffic congestion during toll collection. ALPR system can be used to prevent non-payment at gas station, to control parking of shopping mall and for managing car access among areas. Many developed countries such as, Australia, USA, UK, Germany already deployed these types of applications for the benefit of government and society. Figure 1.2 shows some pictures of real life applications of ALPR system.

### 1.3 Background and Motivation

From the last two decades, ALPR has become a very widespread research topic due to its numerous real-life applications. A basic ALPR system consists of three major steps: image acquisition, LP detection, feature extraction and character recognition. Among these three steps, LP detection is the most crucial stage and the performance of the whole system is highly depended on this. In this detection stage, we need to deal with some important issues such as, hazardous weather conditions, presence of non-LP objects in the background, low contrast LP image and horizontally tilted LP. Collectively all these four issues are identified as hazardous image condition. Figure 1.3(a)-(g) shows some example vehicle images in hazardous condition and Figure 1.3(h) shows a simple vehicle image without hazardous condition.

So far, many efforts have been made to develop high-capable ALPR systems. But they avoid most of the above LP detection issues, which makes those systems very limited at LP detection level. For example, some recent research works are [11], [12], [7], [13], [14] and [6], and all of them avoid the issue of hazardous weather conditions during LP detection level. In [13] the issue of low contrast is considered partially, because enhancement of contrast for the whole image is not always sufficient to detect LP area successfully. Particular afford is needed when an LP region has low contrast problem between LP text and background. In the input image, there can be other non-LP objects. So, efficient filtering of non-LP objects is needed during LP detection. Most of the existing ALPD uses only the LP size, ratio and orientation as criteria for LP filtering, but these are not sufficient. The issue of horizontally tilted LP is considered in [7], but the solution is sensitive to character connectivity. So a complete robust LP detection approach is still needed for making an efficient ALPR system.

### 1.4 Objectives

In this thesis, we give our concentration only on the detection of LP from image. To develop an effective ALPD, we consider the issue of hazardous weather condition, hazardous image background, low contrast image environment and horizontal tilt problem. Specific objectives of this thesis are stated below:

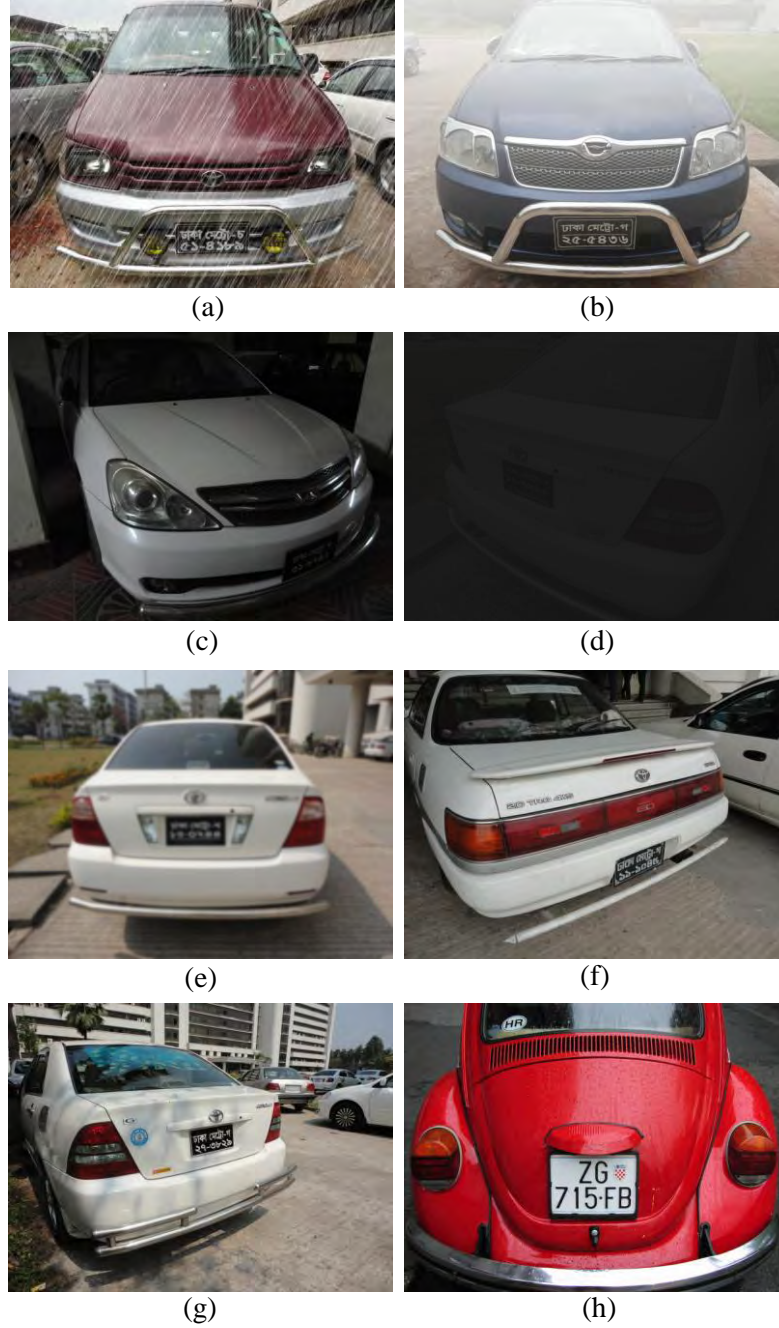


Figure 1.3: Example images of vehicle (a) in rain, (b) in fog, (c) at indoor, (d) at night, (e) having blur effect, (f) having tilted LP, (g) with background objects, and (h) without hazardous condition.

1. Automatic detection of LP considering normal (sunny, cloudy) and hazardous (rainy, foggy) weather condition.
2. Automatic detection of LP from low contrast image (image having low contrast between plate background and text).
3. Provide new conditions for filtering background non-LP objects from LP.
4. Provide an approach for tilt correction of horizontally tilted LP that is not sensitive to character connectivity.

## 1.5 Overview of The Proposed ALPD

It is obvious that a robust and effective ALPD method is required that can detect potential LP area in hazardous condition. In this thesis, we propose a new ALPD method that can detect potential LP area in hazardous condition, as well as, normal condition. Figure 1.4 shows the organization of the proposed ALPD method. The proposed method consists of five stages. In the first stage the input color image is converted to a grayscale image and a noise filter is used to remove small noises from the grayscale image. In this stage, a new approach is introduced for removal of rain streaks from input image. In the second stage, balanced enhancement of contrast is done by using a new approach. This contrast enhancement approach also reduces fog affect from input image. Moreover, a novel statistical method is applied in this stage for binarization. This new binarization method improves the visibility of low contrast LP in the binarized version. In the third stage, the binarized image is processed for cropping the candidate LP regions from image. In the fourth stage, a new method is used to detect the tilt angle for each candidate LP and applied affine transformation to make them correct. Finally at the fifth stage, filtering of non-LP regions are done by using size, ratio and orientation of the candidate LPs. In addition, two new filtering conditions are also applied for filtering non-LPs from candidate LP regions.

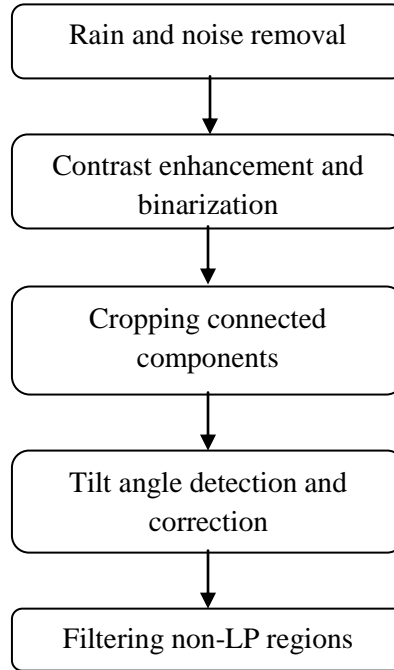


Figure 1.4: Organization of the proposed ALPD method.

## 1.6 Scope of The Thesis

Scope of the thesis is listed as follows:

1. In this thesis, we focus only on automatic detection of LP area from car image. We are not concern about image acquisition and recognition of LP.
2. In this thesis, the center of attention is different hazardous image conditions such as, weather affected image(rainy and foggy), low contrast image (night, indoor, blur), hazardous background and tilted LP (left or right tilt) image. We aim to design an ALPD method that will give better performance for simple input image, as well as, image having hazardous condition.
3. In the issue of weather affected image, we consider only rainy and foggy weather conditions. We avoid snowy and sandy weather conditions because these climate conditions are not happen in our country.
4. In the issue of blur image, we consider only blur affected image due to camera

vibration, but not the motion blur effect. Because high shutter speed image capturing device can solve the motion blur problem.

5. In the issue of tilted LP, we consider only horizontally tilted LP for both left and right directions. Vertically tilted LP is not considered because, mostly a LP is attached with the car body in vertical direction from the ground. So there is a very little chance to have vertically tilted LP in the captured image.
6. In this thesis, we consider input images captured from approximately fixed distance. Because the proposed ALPD needs the knowledge of LP resolution in captured image. Even in practical, many ALPR systems such as, automatic toll collection system, automatic parking allotment system uses sensor triggered image capturing device.

## 1.7 Outline of The Thesis

The rest of the thesis is organized as follows:

In Chapter 2, we briefly describe several supporting technologies and algorithms that we use in our proposed ALPD method. Also the literature review of several existing ALPD techniques are given in this chapter.

The proposed ALPD method is introduced and explained in Chapter 3.

Chapter 4 presents the experimental results, analysis and performance of the proposed ALPD. We also compare our results with two existing ALPD methods.

Finally, some concluding remarks and suggestions for future work are provided in Chapter 5.



## Chapter 2

# Preliminaries and Literature Review

### 2.1 Introduction

The proposed ALPD uses several image processing techniques and methods such as, RGB color to grayscale image conversion, spatial domain filtering, discrete Fourier transformation of an image, entropy measure, Tamura contrast value, Bernsen binarization, binary perimeter image, connected components analysis, morphological erosion-dilation, contrast limited adaptive histogram equalization, Wiener noise filter and Radon transform of an image. In this Chapter, all these preliminaries and basics of image processing are briefly described with examples. Furthermore, a number of existing state-of-the-art ALPD methods are discussed, as well as, highlighted their limitations from the point of hazardous image condition.

### 2.2 Preliminaries

#### 2.2.1 RGB Color to Grayscale Image Conversion

An RGB color image is a collection of three  $M \times N$  size color component images referred to red (R), green (G) and blue (B). At a specific location, each color pixel is a 3-tuple corresponding to the red, green and blue components of an RGB image. The number

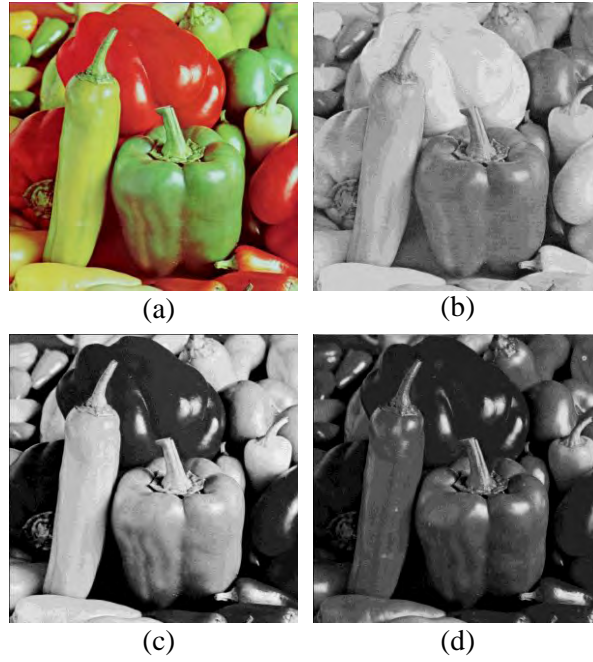


Figure 2.1: An example of (a) RGB color image and its (b) red (c) green and (d) blue color components after decomposition. (Image (a) from [1])

of bits used to represent pixel's intensity value of the component images determines the bit depth of an RGB image. For example, three (R, G and B) 8-bit color component images will form a 24-bit RGB color image. Figure 2.1 shows a 24-bit RGB image and all its three color components.

A grayscale (or gray-level) image is simply a black-and-white image where the darkest color is the black and the brightest color is the white. All the intermediate colors are represented as shades of gray. In a grayscale image, a single intensity value is sufficient for each pixel location. The number of bits used to represent pixel's intensity value determines the bit depth of a grayscale image. In an 8-bit grayscale image, black is represented by 0, white is represented by 255 and intensities from 1 (dark) to 254 (bright) are shades of gray. An RGB color image can be converted into a grayscale image using different weighting of red, green and blue color components [15]. The equation for this conversion is as following

$$Gray(i, j) = 0.30 * R(i, j) + 0.59 * G(i, j) + 0.11 * B(i, j) \quad (2.1)$$



Figure 2.2: An example of 8-bit grayscale image.

where  $(i, j)$  is any pixel location. Figure 2.2 shows the 8-bit grayscale representation of the Figure 2.1(a).

### 2.2.2 Spatial Domain Filtering

Spatial domain means the image surface itself that is composing of pixels and intensity values. Various image processing methods are directly applied on these pixel values for mathematical manipulation. One of the principle spatial domain processing is spatial domain filtering [2] which can be denoted by the expression

$$g(x, y) = T[f(x, y)] \quad (2.2)$$

where  $g$  is the output image,  $f$  is the input image and  $T$  is an operator that is applied on the neighborhood of pixel point  $(x, y)$ . Figure 2.3(a) shows a spatial domain image  $f$  and a neighborhood area centered at pixel location  $(x, y)$ . During spatial domain filtering, the operator  $T$  is performed on the neighborhood of every pixels of the  $f$  image. After filtering process, it will give an output image  $g$  having equal size of  $f$ . Traditionally, the neighborhood is rectangular, centered on  $(x, y)$  and much smaller in size than the image. An example of spatial domain filter is the local mean filter that calculates mean value in the neighborhood area and puts the local mean value at the center pixel of neighborhood. This local mean filter will generate a blurred version of the input image. Another statistical spatial domain filter is local standard-deviation filter that calculates standard-deviation in the neighborhood area. Local irregularities of an input image will be more visible on the output image after applying this filter. Figure 2.3(c)-(d)

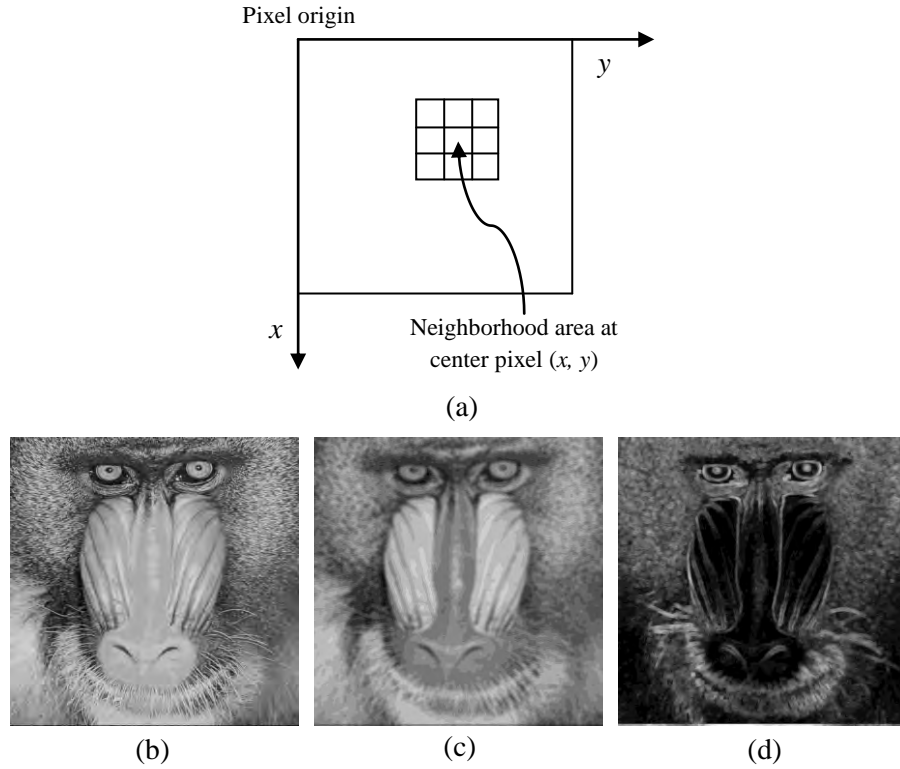


Figure 2.3: (a) Spatial domain filtering, (b) a grayscale image, (c) image after applying local mean filter and (d) image after applying local standard-deviation filter. (Image (b) from [1])

show example images where local mean and standard-deviation filter is applied on the grayscale image of Figure 2.3(b). Here, we consider  $7 \times 7$  pixels area as neighborhood.

### 2.2.3 Discrete Fourier Transform of an Image

An image is a non-periodic discrete function that can be represented as the sum of sines and cosines multiplied by a weighting function [16]. The formulation in this case is the Inverse Discrete Fourier Transformation (IDFT) which is given by

$$f(x, y) = \frac{1}{MN} \sum_{u=0}^{M-1} \sum_{v=0}^{N-1} F(u, v) e^{j2\pi(ux/M + vy/N)} \quad (2.3)$$

where  $f$  is the image,  $(M, N)$  is the resolution of the image  $f$ ,  $x = 0, 1, 2, 3, \dots, M$ ,  $y = 0, 1, 2, 3, \dots, N$ ,  $u = 0, 1, 2, 3, \dots, M$ ,  $v = 0, 1, 2, 3, \dots, N$  and  $F(u, v)$

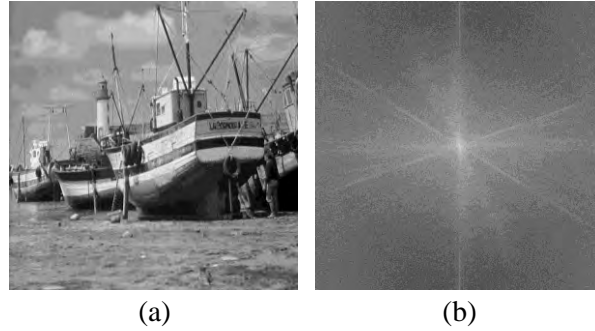


Figure 2.4: (a) Input image and (b) the image after applying forward DFT on the input image. (Image (a) from [1])

is the Fourier coefficient. Fourier coefficients of the image  $f$  can be calculated by using Equation (2.4) which is known as forward DFT of an image. The image composing of all Fourier coefficients is known as Fourier transformed image. Here  $F$  is the Fourier transformed image.

$$F(u, v) = \sum_{x=0}^{M-1} \sum_{y=0}^{N-1} f(x, y) e^{-j2\pi(ux/M + vy/N)} \quad (2.4)$$

The coordinate system of the image  $f$  is covered by  $f(x, y)$  with  $x$  and  $y$  as spatial variables and the coordinate system of image  $F$  is covered by  $F(u, v)$  with  $u$  and  $v$  as frequency variables. We can apply Equation (2.3) as inverse DFT on image  $F$  to get back the initial image  $f$  without loss of information. Figure 2.4(b) shows an example of discrete Fourier transformed image where forward DFT is applied on the image of Figure 2.4(a).

Many regular image-processing tasks such as, smoothing and sharpening are applied on Fourier transformed image using Fourier domain filters. Another important application of DFT on image is reduction of periodic noise. Periodic noise is visible as impulse-like bursts in Fourier transformed image. An use of appropriate mask will remove that visible noise from Fourier transformed image. Finally, the inverse DFT will give the noise removed image.



Entropy value  
= 7.445 bits/pixel

Figure 2.5: An 8-bit grayscale image with its entropy value. (Image (a) from [1])

### 2.2.4 Entropy of an Image

Entropy ( $E$ ) is the measure of average number of bits required to represent an image [17]. As the unit of information for an image is bit, so the entropy will give the measure in bits per pixel. The formula for entropy measure is given as following

$$E = - \sum_{k=0}^{L-1} p_r(r_k) \log_2 p_r(r_k). \quad (2.5)$$

where  $L$  is the number of intensity level and  $p_r(r_k)$  is the probability of intensity level  $r_k$  in that image.  $p_r(r_k)$  can be easily calculated by counting frequency of intensity level  $r_k$ , and dividing it by total number of pixels in that image. Figure 2.5 shows an 8-bit grayscale image of resolution  $512 \times 512$  whose entropy value is 7.445 bits/pixel. The entropy of an image gives the lower bound on the number of bits required to encode its output. In the field of image compression, the lower bound of variable length coding depends on entropy.

### 2.2.5 Tamura Contrast Value

Image contrast means difference of pixel's intensity value in an image that makes distinguishable among different objects during human visual perception. A low contrast image has low visibility of different objects and high contrast image has high visibility of different objects in the image. Figure 2.6(a) shows an example image having moderate level of contrast, and Figure 2.6(b)-(c) shows the low contrast version of the same image.

A well known mathematical measure of image contrast is Tamura contrast value [18].

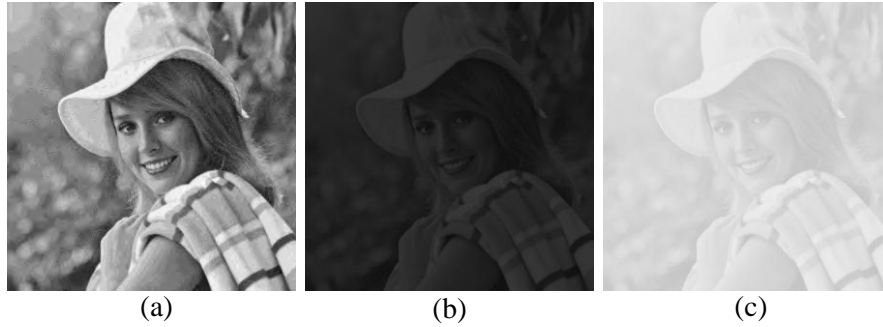


Figure 2.6: Example of images having (a) moderate contrast, (b) low contrast at dark condition and (c) low contrast at bright condition. (Image (a) from [1])

The equation for Tamura contrast measure ( $F_{con}$ ) is given by

$$F_{con} = \frac{\sigma^2}{(\mu_4)^n} \quad (2.6)$$

where  $F_{con}$  is the Tamura contrast value,  $\sigma^2$  is the variance of intensity in the image,  $\mu_4$  is the fourth moment about the mean and  $n = 0.25$ . It gives contrast value within the range of 0 to 1. High Tamura value means high contrast image and low Tamura value means low contrast image. For example, Tamura contrast values of Figure 2.6(a), 2.6(b) and 2.6(c) are 0.29, 0.06 and 0.06, respectively.

### 2.2.6 Bernsen Binarization

Binarization means converting an image into 2-level binary image where the white color is represented as 1 (true) and the black color is represented as 0 (false). A well-known technique for converting a grayscale image into a binary image is Bernsen binarization method [19]. This method uses local thresholding for taking decision during binarization. An advantage of Bernsen binarization is that it shows good performance even in the presence of uneven illumination such as, shadow and exposure.

For measuring local threshold value, Bernsen uses spatial domain filtering where the neighborhood size is  $W \times W$  (a good value for  $W$  is 15). Suppose that  $f$  is the input image and  $f(x, y)$  denotes a gray value at pixel location  $(x, y)$ . The threshold value

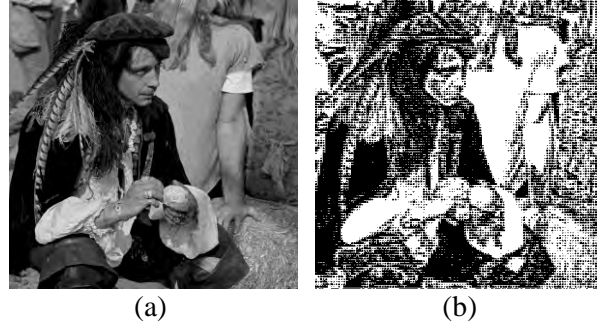


Figure 2.7: (a) An input image and (b) the image after applying Bernsen binarization on the input image. (Image (a) from [1])

$T(x, y)$  of  $f(x, y)$  is calculated by

$$T(x, y) = \frac{\text{maximum in neighborhood area} + \text{minimum in neighborhood area}}{2}. \quad (2.7)$$

Then the binary image is generated by

$$b(x, y) = \begin{cases} 1, & \text{if } T(x, y) > f(x, y) \\ 0, & \text{else.} \end{cases} \quad (2.8)$$

Figure 2.7(b) shows an example binary image that is created after applying Bernsen binarization on the input image of Figure 2.7(a).

### 2.2.7 Binary Perimeter Image

Binary perimeter image contains only the perimeter or boundary pixels of a binary image. To generate binary perimeter image, a simple horizontal-vertical spatial domain filtering and local thresholding method is sufficient. Figure 2.8 shows the filters that will calculate the weighted sum for each pixel of input binary image.

Suppose that  $b$  is the input binary image and  $b(x, y)$  denotes a value at pixel location  $(x, y)$ . The threshold value  $T(x, y)$  of  $b(x, y)$  is calculated by

$$T(x, y) = \text{weighted sum of all values within the filter.} \quad (2.9)$$



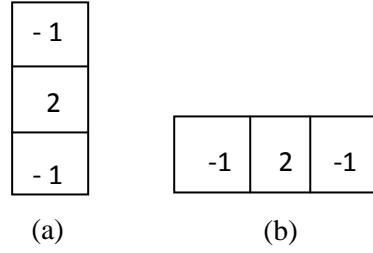


Figure 2.8: (a) Horizontal and (b) vertical filters that are applied on binary image to get the binary perimeter version.

Then the binary perimeter image is generated by

$$b_{peri}(x, y) = \begin{cases} 1, & \text{if } T(x, y) > 0 \\ 0, & \text{else.} \end{cases} \quad (2.10)$$

In this way, the horizontal and vertical filter will generate two separate binary perimeter images that contain horizontal perimeter pixels in one image and vertical perimeter pixels in other. A binary OR operation between these two binary images will generate the target binary perimeter image. Figure 2.9 shows an example binary image and its binary perimeter version.

### 2.2.8 Connected Components in Binary Image

Connected component in a binary image means a white (true) region in the binary image that is connected by n-pixel connectivity [20]. Most often, 8-pixel connectivity is used to detect connected components where a white pixel considers all its surrounding 8 pixels as neighbor. A binary image can have zero or number of connected components. Traditionally, each connected component is labeled with an integer. Figure 2.10 shows a binary image and its connected components with integer labeling. A simple way for finding connected components is Depth First Search (DFS) algorithm where all the white pixels are considered as vertices of a graph and 8-pixel connectivity is adjacency of a vertex.

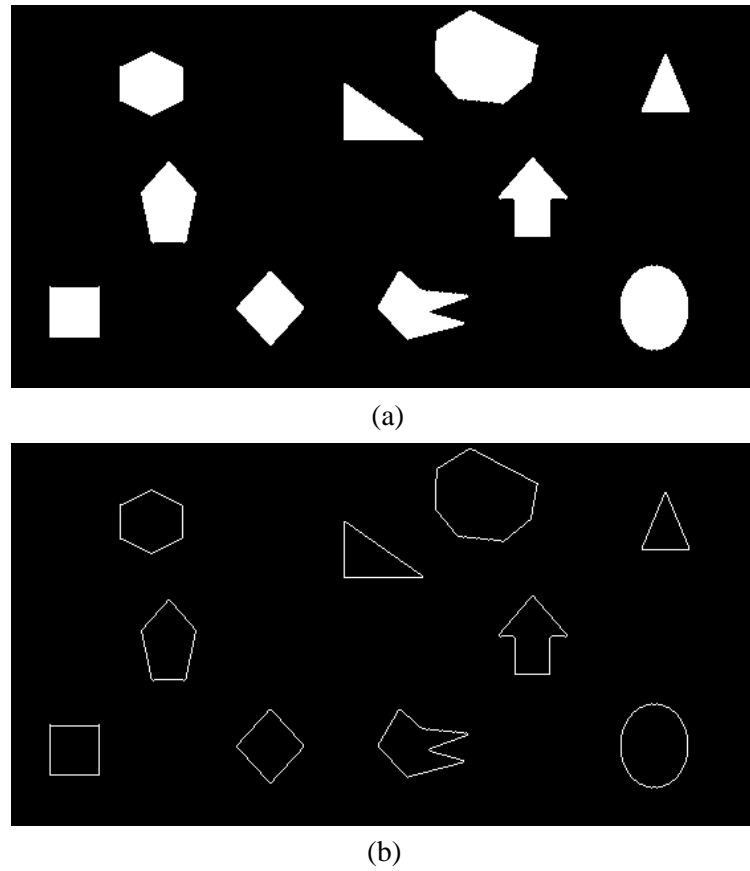


Figure 2.9: An example (a) binary image and its (b) binary perimeter version.

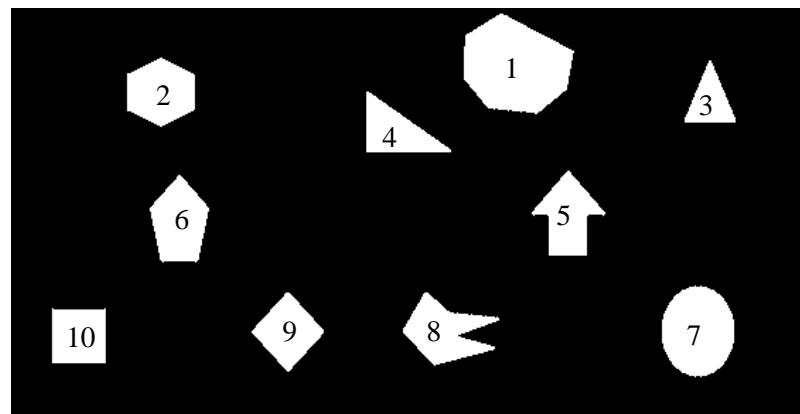


Figure 2.10: An example binary image that contains 10 connected components.

### 2.2.9 Contrast Limited Adaptive Histogram Equalization

Histogram of an image is simply the distribution of different intensity values in the image. A high contrast image has flat or uniform distribution of intensities. That

means histogram of high contrast image covers a wide range of intensity scale. On the other hand low contrast image has narrow histogram. Figure 2.11 shows some images with their histogram.

Histogram Equalization (HE) is a common technique for enhancing contrast of an image. It uses mathematical transformation function that will automatically improve the contrast of an image by stretching the narrow distribution of image intensities. When an HE method utilizes the whole histogram of an image at a time, then we can say it Global Histogram Equalization (GHE). But GHE doesn't work well all the time because sometimes it generates image having washed-out appearance. Figure 2.12(a) shows a low contrast image of a Mars rock and Figure 2.12(b) shows the contrast enhanced version of that image after applying GHE. Image of Figure 2.12(b) has unwanted washed-out appearance. A better method of HE is Adaptive Histogram Equalization (AHE) where an image is divided into overlapping or non-overlapping blocks. Histogram of each block is processed separately for equalization. But in non-overlapping AHE there can be blocking artifacts in the output image, and in the overlapping AHE the running time is not cost effective. Another disadvantage of AHE is that it over-amplifies noise in moderately uniform regions of an image. An improved version of AHE is Contrast Limited Adaptive Histogram Equalization (CLAHE)[21], which is faster due to non-overlapping block process and there is no blocking effects due to linear interpolation at block boundary. In CLAHE, we can control the contrast enhancement limit by clipping the histogram at a predefined value before computing the transformation function. A good choice for contrast limit is 0.01. Figure 2.12(c) shows the resulted image after applying CLAHE on the image of Figure 2.12(a).

### 2.2.10 Morphological Erosion and Dilation

In morphological image processing, two common operations for binary image are erosion and dilation [22]. Morphological erosion of a binary image means shrinking or thinning of white (true) regions. Amount and shape of the thinning depends on Structuring Elements (SE). Morphological operations are based on how this SE fits or misses the shape of the white regions. During erosion, the center pixel of an SE is placed on every pixels of a white region. If the SE fully fits in the white region for that particular pixel

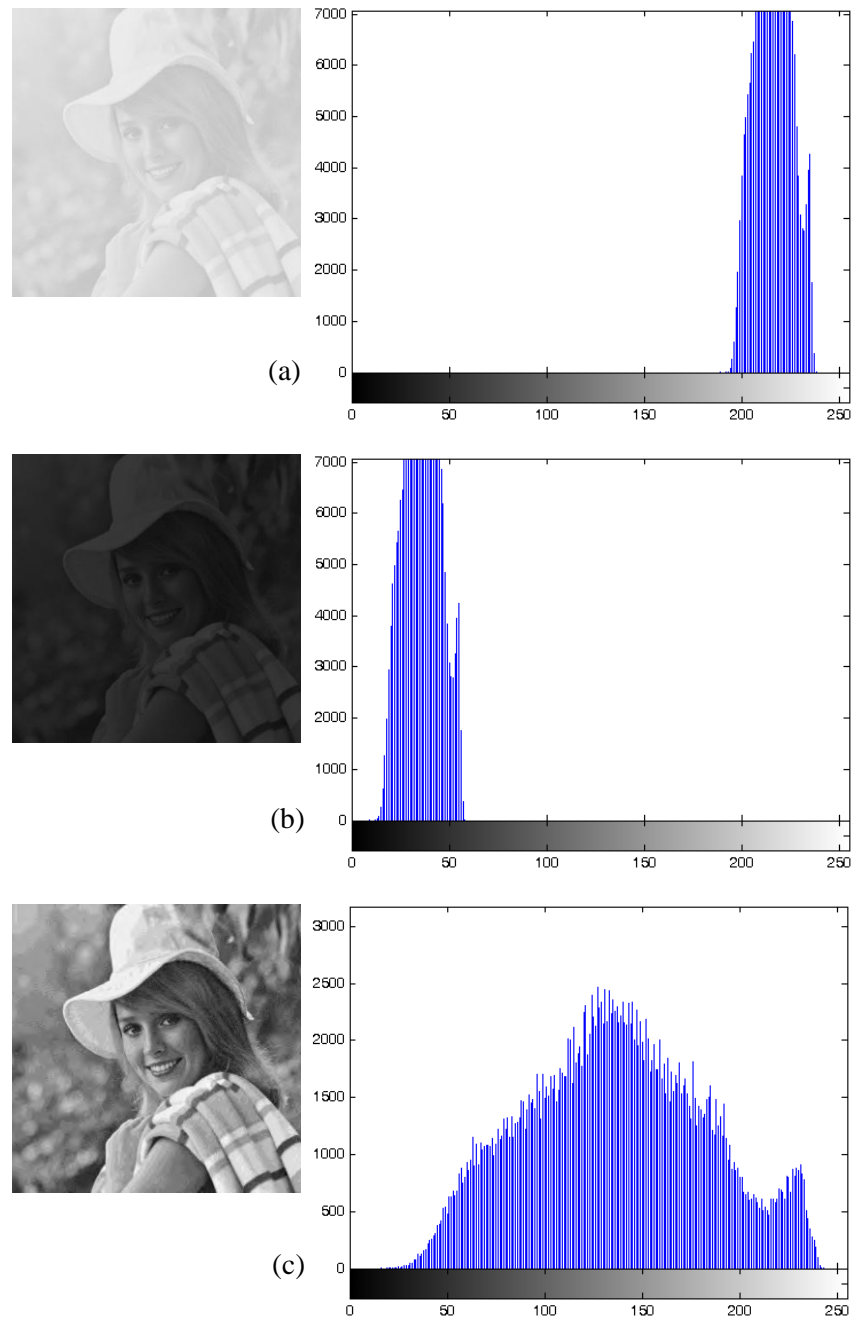


Figure 2.11: Examples of images having (a) low contrast at bright condition, (b) low contrast at dark condition and (c) high contrast. Individual histogram is placed at the right side of each image.

position, then the pixel remains in the binary image. Otherwise SE will put 0 (false) in that pixel position. Figure 2.13 shows an SE element and the resulted image after

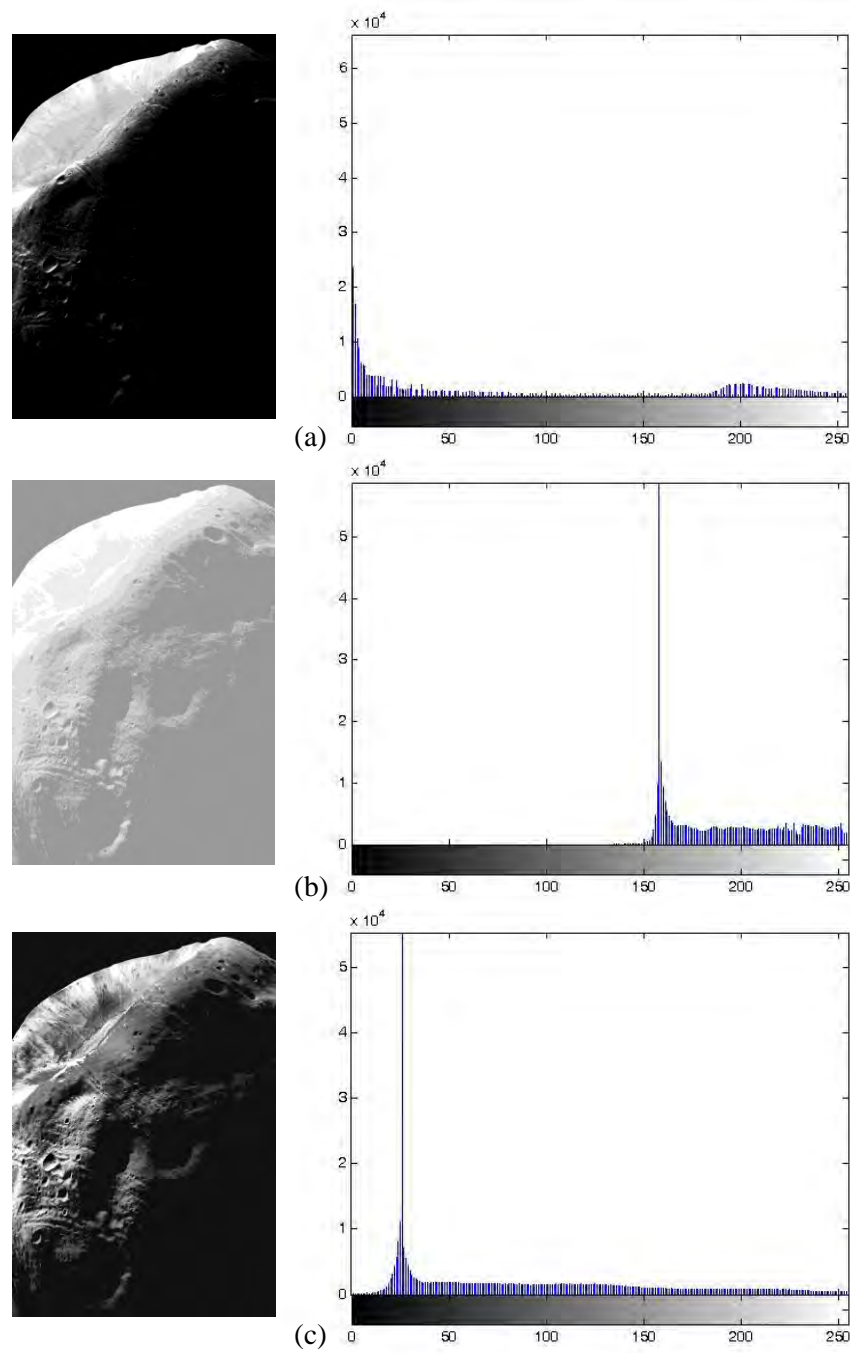


Figure 2.12: Example of (a) low contrast image, (b) resulted image after applying GHE and (c) resulted image after applying CLAHE. Individual histogram is placed at the right side of each image.(Image (a) from [2])

applying morphological erosion with that SE. Morphological dilation of a binary image means growing or thickening of white (true) regions. Like erosion, amount and shape

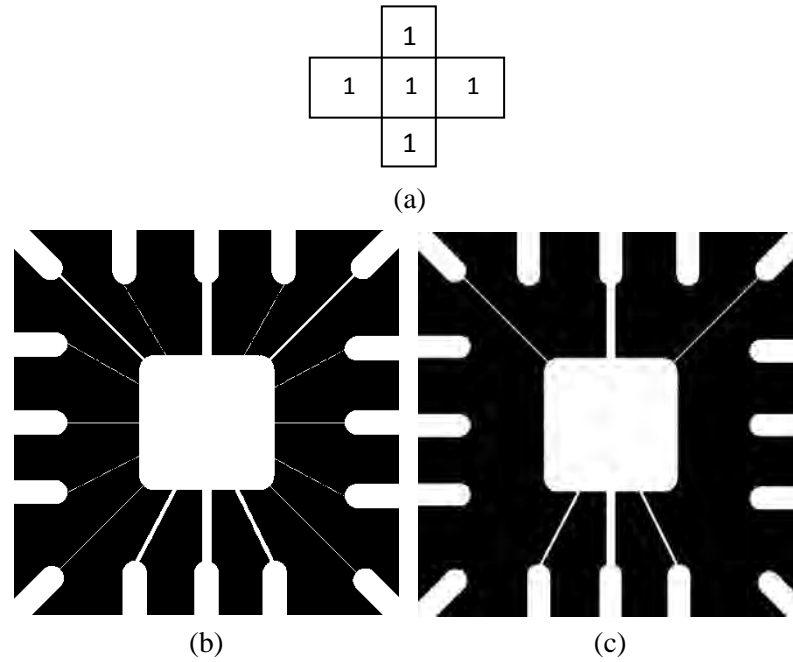


Figure 2.13: (a) Structuring element that is applied on the (b) input binary image. After erosion, several thin lines are removed from (c) the resulted image. (Image (b) from [2])

of the thickening depend on structuring elements (SE). During dilation, the center pixel of an SE is placed on every pixels of a black (false) region. If the SE overlaps with any part of the white regions then SE will put a 1 (true) in the center position of it. Otherwise SE will put zero (false) in that pixel position. Figure 2.14 shows an input binary image and the resulted image after applying morphological dilation with the SE of Figure 2.13(a). Morphological erosion followed by dilation can be used for small noise removal, removing trivial connectivity between connected components and smoothing shape of a white region in the binary image.

### 2.2.11 Radon Transform of an Image

Radon transformation of an image is the projection of image intensity on a projection line having specific angle. Projection can be calculated by simply adding intensity values of the image in the perpendicular direction from projection line. In Figure 2.15, a binary image is given and the projection of this image is reflected on  $45^\circ$  and  $-30^\circ$  lines. Here,

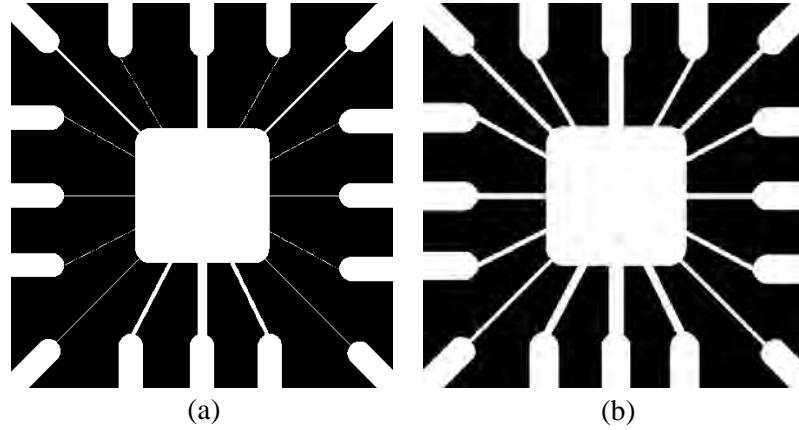


Figure 2.14: (a) The input binary image and (b) the resulted binary image after dilation. Same structuring element of Figure 2.13(a) is used for 3 times to increase the thickness. (Image (a) from [2])

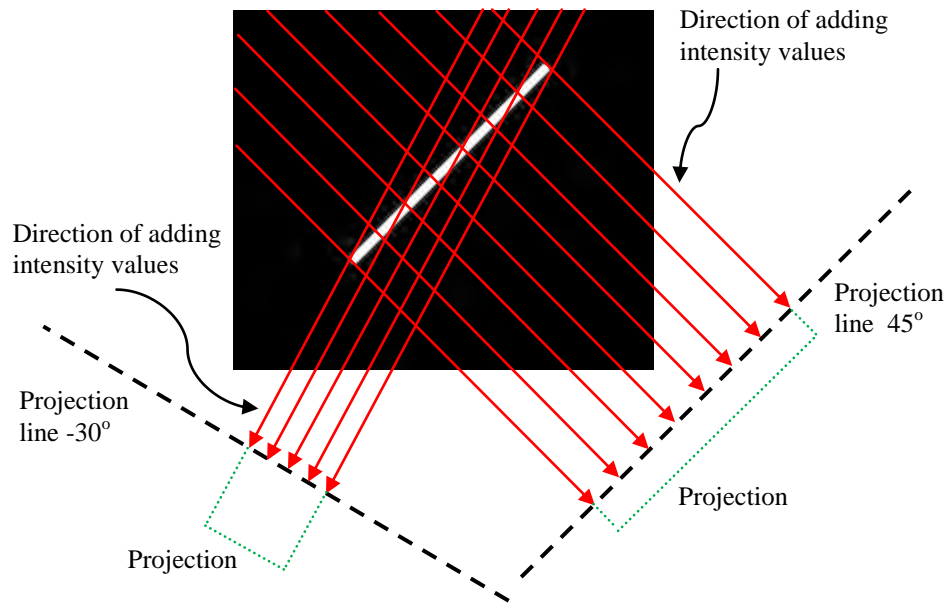


Figure 2.15: Projection of a binary image on +45 degree and -30 degree projection line.

the dashed black line is the projection line, the red arrows (perpendicular to projection line) are the direction of adding intensity values and the green curve on the projection line is the projection area with amplitude. In this way, for a range of projection line orientations, we can do Radon transformation and get a Radon transformed image or a 2D-matrix. The number of rows in the transformed image depends on the number of pixels in the diagonal of the input image and the number of columns depends on

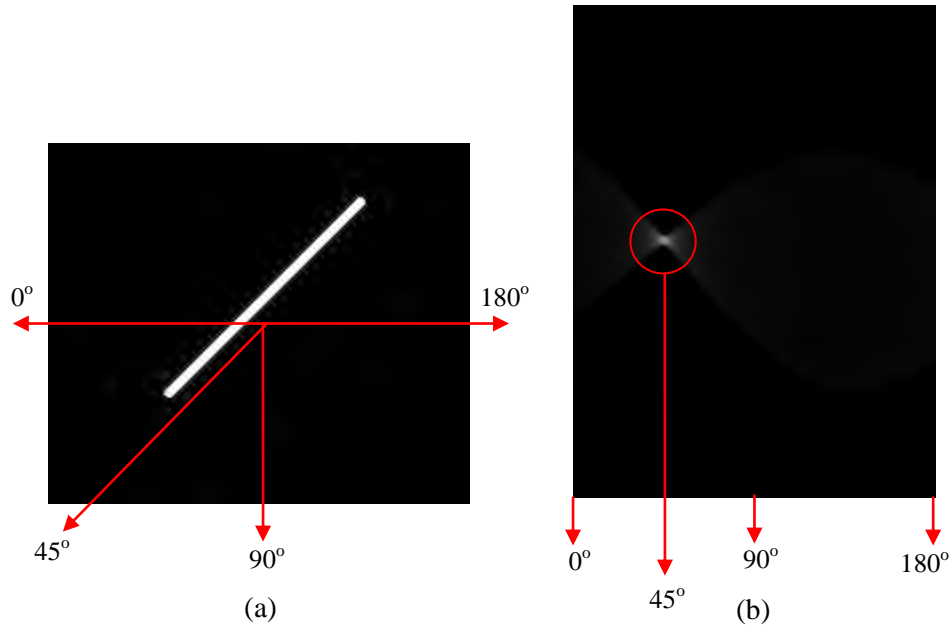


Figure 2.16: (a) A binary image where the white component have 45 degree orientation and (b) the bright spot located at 45<sup>th</sup> column of the Radon transformed image.

the range of projection line orientations. Figure 2.16(b) shows the Radon transformed version of the binary image of Figure 2.15. Here, we consider -90 degree to +90 degree orientations of projection line. The resolution of the output Radon transformed image is 277 (diagonal length of the input image) by 181 (from 0° to 180°). In Figure 2.16(a), the orientation of the white object is 45 degree. During Radon transformation, when the projection line orientation is -45 degree then the projection area of the white object is small but highly concentrated. This phenomenon is reflected in the Radon transformed image where a bright white spot is found at 45th column (degree) location. So it is possible to find the dominant direction [23] of a binary image by finding the maximum bright spot in the Radon transformed image.

### 2.2.12 Wiener Noise Filter

For filtering noises, one of the most primitive and well-known technique is local Wiener filter [24]. It uses neighborhood of size  $m \times n$  to estimate the local mean and standard deviation of the image. Where the standard deviation is high, Wiener performs little smoothing and where the standard deviation is low, Wiener performs more smoothing.



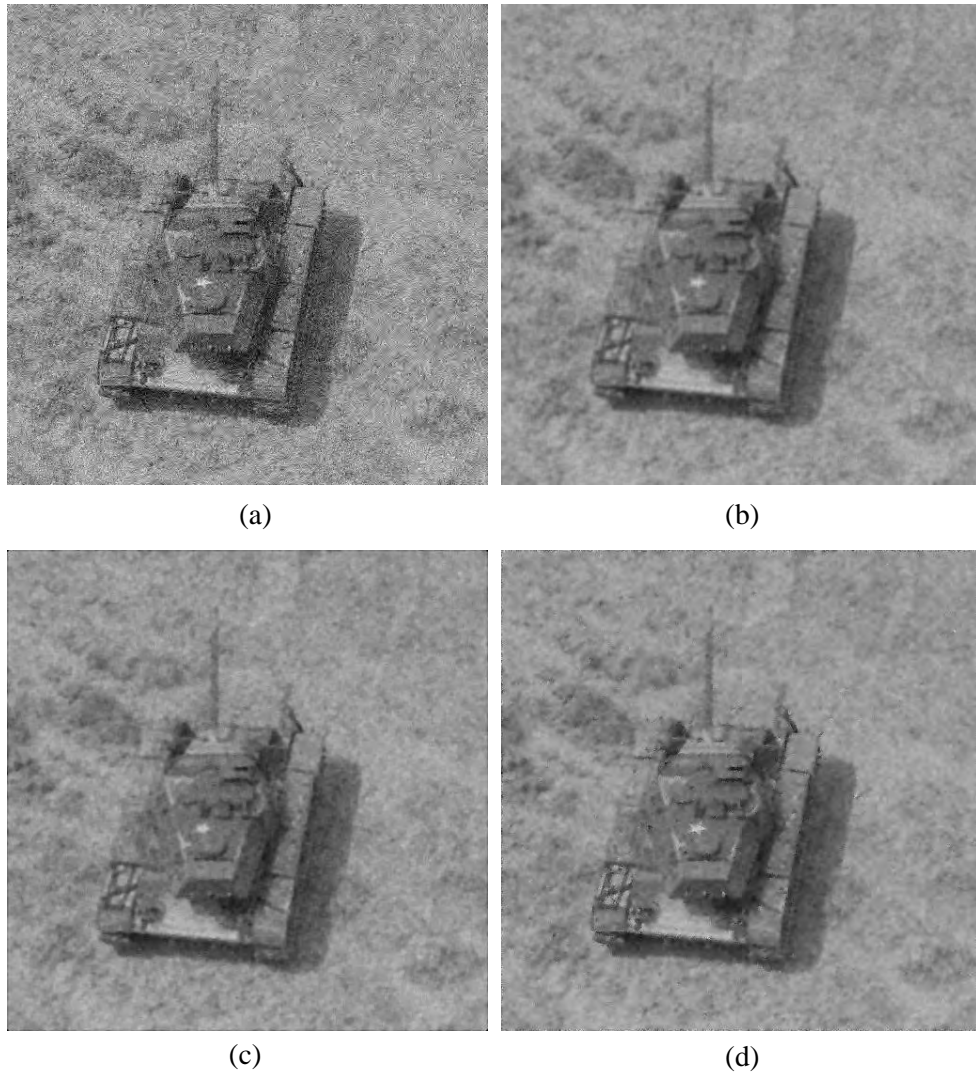


Figure 2.17: (a) A noise induced grayscale image, and the images after using (b) Gaussian noise filter, (c) median filter and (d) Wiener noise filter.

This filter works better than local Gaussian filter and median filter, because Wiener filter protects edges and other high frequency parts of an image. Figure 2.17 shows a grayscale image that is artificially induced by Gaussian noise and the images after using Gaussian, median and Wiener noise filters. Neighborhood size of  $5 \times 5$  is used in all filters. If we closely observe the Figure 2.17(d), then we can see less blur effect than Figure 2.17(b) and 2.17(c).

## 2.3 Literature Review

From the last decade, many efforts have been made to solve the problem of detecting potential LP area from image. Different state-of-the-art methods apply different image processing approaches, techniques and algorithms to build their ALPD methods. To detect LP area from an image, different features such as, geometric feature, texture feature and color feature are utilized individually or jointly [9]. A simple geometric feature of an LP is the rectangular shape of the LP boundary. But this feature is sensitive to unwanted horizontal-vertical edges and hardly applied for tilted LP. Other geometric features are the size, ratio, and orientation of an LP. However, these features are highly depends on distance and angle of capturing image. Texture feature means frequent intensity transition inside LP region due to characters. In other words, local-irregularity or edge-density is high inside LP due to presence of text. But it produces detection errors when there are other text-regions in the image. Color feature is the color pattern of LP text and background. But this feature is highly sensitive to illumination condition and noises, as well as, depends on LP color standard of different countries. Combining two of more features is effective for ALPD, but it is computationally complex and costly.

During detection of LP, we need to consider several unavoidable image issues such as, images affected by weather conditions (rain, fog), image having low contrast environment (night, blur, indoor), image having horizontally tilted LP region and image background having other objects. These issues are collectively considered as the hazardous conditions of an image. Hazardous conditions have the effect on the above mentioned features of an LP and thus increases the LP detection error. Presence of rain streaks in image creates unnecessary irregularities and edge density. This unnecessary texture feature increases the number of plate like non-LP regions. As a result, a non-LP region can be wrongly detected as target LP region. Even, occurrence of rain streaks inside LP region creates problem at the character segmentation stage of an ALPR system. So removal of rain streaks is necessary at the initial stage of an ALPD. An input image for ALPD can be affected by low contrast environments such as, fog, low illuminated night, indoor, and blurriness. These low contrast environments degrade the visibility of LP

texts, LP rectangular boundary edges, and LP foreground-background color difference. That means, it affects the geometric, texture and color features of an LP. Therefore, improving visibility by contrast enhancement is important for an ALPD. Due to camera position and angle, an LP region can be horizontally tilted in the captured image which affects the geometric feature of an LP region. Consequently, it makes difficult to detect LP region based on geometric feature. In the captured image, there can be other objects (such as, headlight, bumper, car logo and many others) in the image besides LP. Here, the target LP is the foreground and the other objects are the hazardous background. Hazardous background creates ambiguity for ALPD to select the original LP region. To locate the target LP, effective filtering is needed using LP features.

During our review we find that existing ALPD methods does not consider the hazardous conditions fully. Several state-of-the-art ALPD techniques are briefly described below with their underlying techniques and limitations from the view of hazardous conditions. In [25], Anagnostopoulos et al. present a license plate recognition system for the LP written in English. The ALPD stage of this system takes grayscale image as input and apply a segmentation technique called Sliding Concentric Window (SCW) to select texture rich area from the image. Then it uses Sauvola binarization method to binarize the image and do connected component analysis (CCA). In the CCA, non-LPs are rejected based on ratio, orientation and counting Euler's number. But Euler's number inside LP region is highly sensitive to small white noises. Even, no noise filter is used in any stage of the ALPD method. This ALPD method does not consider the weather effect, tilted LP and low contrast image environment. No such special attempt is taken to resolve these problems. It works well only for simple images having no hazardous condition.

In [26], Huang et al. propose an intelligent way to inspecting annual status of motorcycles based on LP detection and recognition. In the ALPD stage, first the grayscale image is binarized using Otsu thresholding and then a  $3 \times 3$  median filter is applied to remove noises. To detect edges from the noise removed image, Prewitt operator is applied. After that, horizontal histogram analysis is applied to segment a horizontal portion from the image that contains the potential LP region. On the horizontally segmented area, vertical histogram analysis is used to find a high dense rectangular area

(LP area). To filtering non-LP regions, they use only the ratio 3 by 1 (straight LP) and, horizontal counting of intensity transition (black to white or white to black) inside LP region. However, for filtering non-LP regions this approach is not applicable when the LP region is horizontally tilted. Because when we consider tilted LP, the ratio varies and, horizontal counting needs tilt corrected LP to give good filtering results. In [26], the ALPD for motorcycles does not consider any weather effects, low contrast problems and horizontal inclination of LP.

In [27], Kaushik et al. present an ALPD method for Korean cars. To find the region-of-interest (LP area), it uses an improved version of SCW [25] that detects horizontal and vertical edges. After that, based on the shape and size of an LP, only the rectangular regions are kept in the edge image. Finally, connected components are extracted from the image and filtered all the non-LPs based on aspect ratio and color information. One of the limitations of this ALPD method is the use of rectangular edge information of an LP for initial detection because, it is not always possible to detect significant LP edge information from image when there is low contrast between plate and car-body. Even rectangularity of an LP is violated when the LP region is horizontally tilted. Another limitation is that color information of an LP region is sensitive to uneven illumination and low contrast. So use of color information will lead the ALPD approach to a wrong selection of LP during filtering. Also this method avoided the issue of weather effect, low contrast and tilted LP.

In [12], Ashim et al. propose a license plate recognition system for the LP written in Bangla. The ALPD stage of this system takes grayscale image as input, applies GHE for contrast improvement and median filter for noise removal. Then Sobel vertical operator is used to detect vertical edges from the image. To extract candidate LP region from the image, thresholding is used to select rows based on edge density. Morphological erosion and dilation is applied on the selected rows to remove unrelated objects. Finally, potential LP region is found using vertical cut based on edge density. To remove fake regions, they use only the aspect ratio as filtering criteria. In this ALPD technique, there is no concern of weather effect and tilted LP issues. Even, no analysis is given for handling night and blur image. At the beginning stage, it uses GHE for contrast enhancement and median filter for noise filtering, but this techniques show questionable

performance (see section 2.1.9 and 2.2.12). Another limitation is use of edge density and threshold value (histogram analysis) for horizontal cut. Because an image may contain other objects having high edge density, and so, it incorrectly makes a large horizontal cut when multiple objects overlap. A better approach is CCA instead of using histogram analysis.

Joarder et al. [13] present another Bangla LP detection method which is based on vertical edge density. This ALPD method uses edge density to enhance the local contrast. Contrast of a high dense region increases more than a low dense region. However, this contrast enhancement approach fails when there is weak edge information inside LP area (suppose night and blurry image). Another problem is that no noise filter is used before using the contrast enhancement approach. Thus contrast enhancement increases noises of the image. To detect candidate LP regions, it considers rectangular high dense regions as target area and uses a plate like match filter to find the location. After that filtering using size and aspect ratio is applied to select potential LP regions. In this ALPD, no such approach is given to handle the issue of tilted LP, weather conditions and, low contrast night and blur image.

In [6], Mahmudul et al. present a real time license plate recognition system for the license plate written in Bangla. The ALPD stage of this system takes grayscale image as input. So the input color image is converted to grayscale image first. From this grayscale image they produce an edge image using Canny edge detector. This edge image is further processed to detect the LP region. To detect the LP region the ALPD stage uses two major steps. The first one is finding the possible location of the vehicle in the image using symmetric property of the vehicle. If we see a vehicle from front or rear, then it will be symmetric along a vertical axis. The idea of symmetry property of a vehicle was first introduced in [28] for detecting on-road vehicles. To detect the vertical axis of symmetry in the image, it uses a large window having three-fourth height and one-fourth width of the edge image. The center column of the window is considered as the vertical axis. For each point on this vertical axis, a value is computed by adding up the absolute differences among the mirrored pixels equally separated by the axis. In this way for each column of the input image, the large window is convolved and values are stored into another matrix called symmetry matrix. In the symmetry matrix, we



Figure 2.18: Example of (a) an input grayscale image, (b) it's edge image. The white vertical line in the edge image is the axis of symmetry which intersects the LP region of the image.

select a column as the vertical axis of symmetry whose sum of values is the minimum. Most of the cases, this vertical axis of symmetry intersects the LP region of the image. Figure 2.18 shows an input grayscale image and its edge image version with vertical axis of symmetry (the vertical white line). In the second step, the target is to find the rectangular boundary of LP region on that vertical axis of symmetry. It starts from the bottom of the vertical axis and search for a white pixel on it. When a white pixel is found on the vertical axis, it means, it can be the crossing point between the lower-edge of the LP and the vertical axis. This point is named as Probable Crossing Point (PCP). Then a small window of size  $IW$  traverses at the right direction of the PCP, until it finds an area without any white pixel. In this way it will get the approximate bottom-right point of the LP. On that horizontal line (from PCP to bottom-right point), they search a point that has the maximum number of white pixels above it. Now from that point, again a window searches the top-right point. Similarly, it searches the left-top point of the probable LP region. At any stage, if the search fails to get any LP edge points, it will restart the search from next PCP point. Finally, a detected rectangular region is considered as valid LP region if it fulfils the target aspect ratio and size. Figure 2.19 shows an edge image with localized LP region. A major limitation of this ALPD method is the symmetry property which is sensitive to tilted vehicle image. Because inclined vehicle have no symmetry property, thus give wrong vertical axis of symmetry. For low

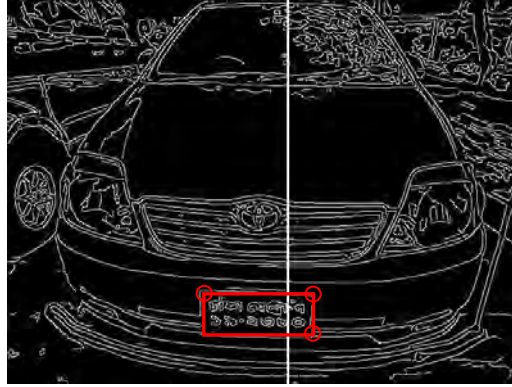


Figure 2.19: Example of edge image with vertical axis of symmetry. The red marked box contains the detected LP region. Small circles on the box are the points found during LP search on vertical axis of symmetry.

contrast image, it is not always possible to have proper rectangular region of LP in the edge image. Boundary can be broken due to low intensity difference between car body and the LP background color. In this ALPD method, original LP region is filtered using only size and ratio. But these two features are not sufficient for good filtering of non-LPs. This method works well when there is no inclination and the surrounding LP region has less density of edges. Another limitation is that no noise filter is used in any stage of the ALPD. However, noise can mislead the detection of PCPs. Also this method avoided the issue of weather effects and low contrast image.

Yem et al. [7] present an automatic vehicle license plate recognition system for Chinese LP. The ALPD stage of this system has the ability to handle uneven illumination, particularly the shadow. To remove shadow from the input grayscale image, it uses a novel improved Bernsen binarization method. Let denotes the input grayscale image as  $F1$ . In the improved Bernsen method, a Gaussian filter is applied on  $F1$  image and generates a smoothed version  $F2$ . Then Bernsen threshold matrix for both image  $F1$  and  $F2$  are calculated using Equation (2.8). Let denotes the threshold matrix for image  $F1$  as  $T1$  and for image  $F2$  as  $T2$ . The shadow removed binary image is obtained by

$$b(x, y) = \begin{cases} 0, & \text{if } F1(x, y) < \beta ((1-\alpha)T1(x, y) + \alpha T2(x, y)) \\ 1, & \text{else.} \end{cases} \quad (2.11)$$

where  $\alpha$  is a parameter to adjust the balance between the traditional Bernsen algorithm



Figure 2.20: (a) An example LP region affected by shadow, (b) after applying Gaussian smoothing filter, (c) output of traditional Bernsen and (d) output of improved Bernsen.

and the improved Bernsen algorithm. If  $\alpha$  is 0 then it becomes the regular Bernsen algorithm. Choosing the appropriate value of  $\alpha$  can effectively remove the shadow. Experimentally to get best results, the value of  $\alpha$  is set to 0.5,  $\beta$  is set to 0.9 and size of the local neighborhood window is  $1 \times 19$ . Finally median filter is applied to remove noises. Figure 2.20 shows a cropped LP region and the Gaussian smoothed version. Binary versions after applying the traditional and improved Bernsen binarization method are also given in Figure 2.20. After removing the shadow, the binary image is further processed to detect the LP area. To detect each individual white region, they apply 8-neighbor connected component analysis. If an LP has black characters on white background, then the white frame of the LP will detect as a connected component. This component is nominated as LP, if the size coincides with plate size. But there can be other plate-sized components in the image which are not the original LP. To filter non-LPs, each component is scanned at the midline and count number of intensity transition. Based on the counting value, non-LP frames are efficiently filtered. If an LP has white characters on black background, then no frames will be detected as LP. In this situation, the LP is detected by large numeral extraction. First, components having small size (than large numeral in the LP) and unmatched ratio are removed from the binary image. Second, to remove some non-character components, average distance between characters is also used as filtering condition. In this way, unnecessary connected components are removed from the binary image and only the numeral connected components are preserved. Finally, a group of numeral connected components are cropped from the image which is the potential LP region. This ALPD method has the horizontal tilt detection and correction approach. Inside the detected LP region, characters are localized as binary connected components and find the center position of each. Then the tilt angle is computed by averaging the tilt angle of every two central points. In this ALPD method,



Bernsen binarization is used which is sensitive to noise. It creates unnecessary character connectivity in the binarized image and thus multiple numeral characters become one horizontally longed component. This fact will mislead the ALPD by removing multiple connected numeral characters from the binary image due to unmatched ratio. Even this phenomenon causes wrong detection of LP tilt angle. It can be happen that all the characters inside LP region are connected due to noise and generate one connected component having one center point. Thus tilt angle detection is not possible using one point. Presence of noise also misleads the filtering process. During filtering, each component is scanned at the midline and count number of intensity transitions. Based on the counting value, non-LP frames are filtered. However, noise on the midline changes the counting value and may create wrong selection.

In [11], Wang proposed an ALPD method based on Discrete Wavelet Transform (DWT) and sliding window. DWT is used to decompose the input grayscale into four subbands Low-Low (LL), High-Low (HL), Low-High (LH) and High-High (HH). The HL and LH subband contains only the vertical and horizontal details of an image, respectively. In this ALPD, both HL and LH subband is used to detect the LP location. First, to remove unnecessary details from LH and HL subbands, horizontal and vertical histogram analysis is used. In vertical and horizontal histogram, thresholding is applied to remove insignificant rows and columns from LH and HL subbands respectively. After that the target LP is localized based on number of intensity transition and its boundary region is fine-tuned using a sliding window. This ALPD method fails when there are unclear edges due to low contrast image environment (night, blur and fog). The ALPD have no steps to handle unnecessary edges due to rain drops, as well as, no approaches to handle horizontally tilted LP and noises. Moreover, only the edge-density is used to localize an LP, which is not a sufficient feature for detecting LP in hazardous background issue. In [14], Hsu et al. present an application oriented ALPR system where parameters are adjustable to place the system in three different applications: access control, law enforcement and road patrol. At the ALPD stage, it uses vertical edge clustering method to detect edge dense regions from the image. All these edge dense regions are the candidate LP regions. Finally non-LP regions are rejected based on size, orientation and aspect ratio. This ALPD method has no approaches for rain removing and enhancing

<i>Ref.</i>	<i>Weather condition</i>	<i>Horizontally tilted LP</i>	<i>Low contrast</i>	<i>Filtering Criteria</i>
[25]	No	No	No	ratio, orientation, Eulers number
[27]	No	No	No	ratio, color
[26]	No	No	No	ratio, horizontal counting
[11]	No	No	No	horizontal counting
[7]	No	Yes, but sensitive to character connectivity	No	size, ratio, horizontal counting
[12]	No	No	Use GHE, but not effective always	ratio
[13]	No	No	Yes, but not effective always	ratio, size
[6]	No	No	No	ratio, size
[14]	No	No	No	orientation, ratio, size

Table 2.1: Consideration level of four hazardous conditions in different state-of-the-art ALPD methods.

low contrast image. However, rain streaks increase irrelevant edges and low contrast environment decreases visibility of sharp edges in the image. Thus, it will mislead the edge clustering method and degrade the performance of detecting potential LP regions.

## 2.4 Conclusion

In this chapter, we discuss several preliminary image processing techniques which are utilized in different stages of our proposed ALPD method. Several existing state-of-the-art ALPD methods are reviewed and given comments on their ability to detect LP in hazardous conditions. In Table 2.1, we mention the consideration level of hazardous conditions for different existing ALPD methods. We see that none of the existing ALPD methods are able to handle the issue of weather condition. The issue of horizontally tilted LP is considered by one [7] of them, but the solution is sensitive to character connectivity and noises. All others are considered zero-tilted or trivially-tilted LP. That's why they have no such special approach to handle tilted LP. Most of the existing ALPD methods [11, 7, 14, 6, 25, 26, 27] consider input images having good contrast and illumination.

So they do not have any contrast enhancement step in their ALPD. Only [12] and [13] use contrast enhancement approach to enhance overall contrast of the image which is not effective for very low contrast (night and blur) LP region. During filtering of non-LP regions from background, most the existing methods use LP size, ratio, and orientation as filtering conditions. In [25], Euler's number (total number of white objects minus holes) is used as a condition for filtering LP, but it fails when noise increases or decreases unwanted white objects. Even, some ALPDs [11, 7, 26] use counting of horizontal intensity transition in binary LP region as filtering condition without using any noise filter beforehand. Color of an LP can be used as a criterion for filtering LP [27], but it is sensitive to illumination. So additional filtering criteria are still needed for effective filtering. Overall, all the existing ALPD methods are very limited if the matter of hazardous image conditions are judged.

## Chapter 3

# The Proposed ALPD

### 3.1 Introduction

In the previous Chapter, we discuss about several existing ALPD methods. But most of the existing methods are partial or imperfect to handle hazardous image conditions. Motivated by this fact, we propose a new ALPD method that detects LP in hazardous condition. In this chapter, we describe the details of the proposed ALPD. The proposed ALPD method comprises of five stages and each of them is involved to handle the issue of hazardous conditions. Several new approaches are introduced at different stages of the ALPD. Specific purpose, intuition and explanation for each of these new approaches are stated broadly in this Chapter.

### 3.2 The Proposed ALPD Method

The proposed ALPD method consists of following five major stages,

1. Grayscale conversion, noise and rain effect removal,
2. Contrast enhancement and binarization,
3. Local counting filter and Cropping Connected Components (CCC),
4. Tilt angle detection and correction,
5. Filtering non-LP regions.

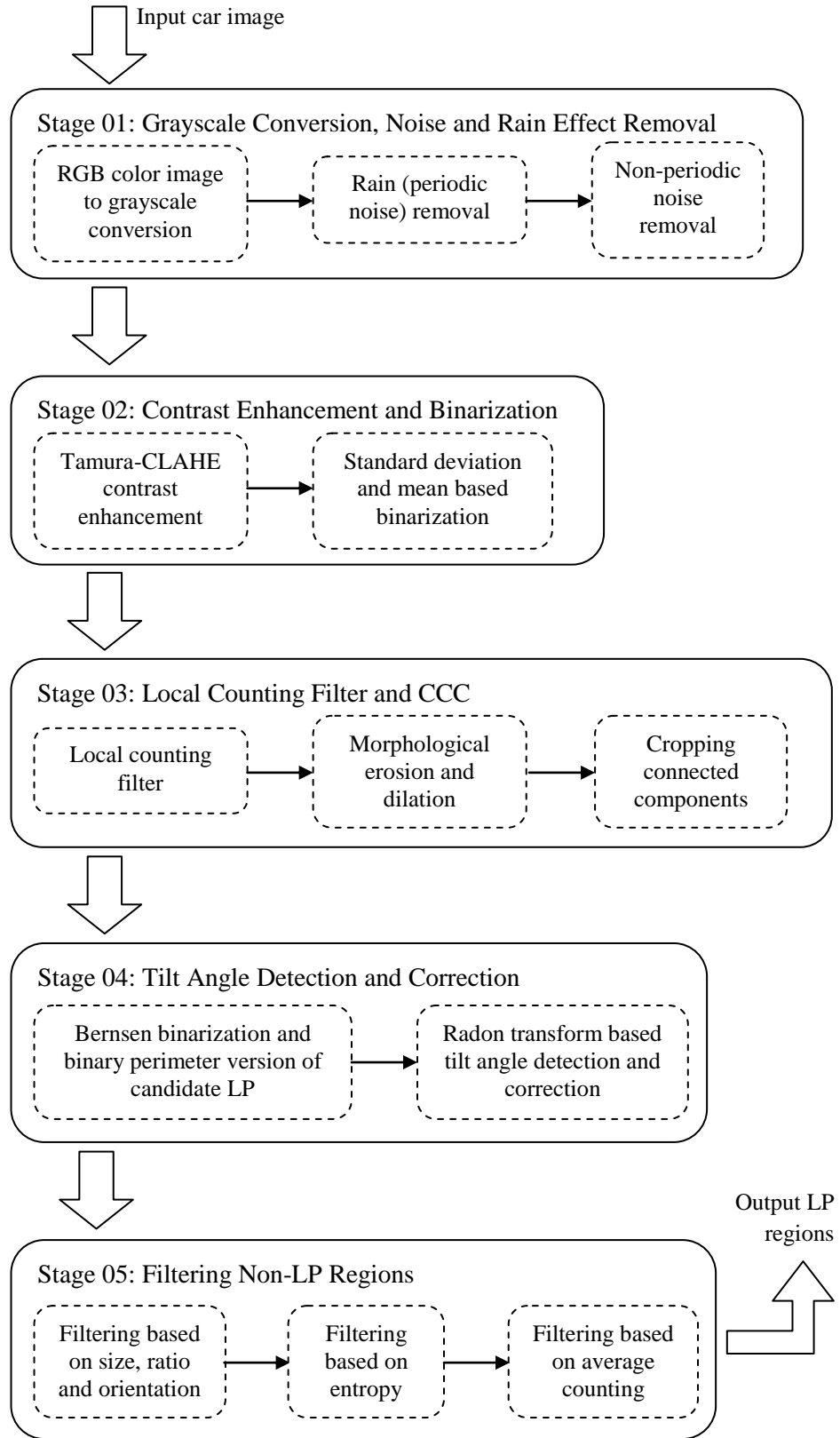


Figure 3.1: Sequential stages of the proposed ALPD method.

In most of the stages, new approaches are introduced which makes our proposed ALPD system significantly different than other existing solutions. Figure 3.1 shows the sequential stages of the proposed ALPD method. At the first stage, we convert the input (RGB color) image into a grayscale image, as well as, remove periodic noises (Rain) and non-periodic noises from the grayscale image. This noise removed grayscale image is the input for the second stage. In the second stage, we apply Tamura-CLAHE contrast enhancement to improve the visibility of indoor, night, blurry and foggy images. A new binarization method (based on local standard deviation and mean) is also applied on the contrast enhanced grayscale image to generate a binary image. This binary image is the input for the third stage. In the third stage, a local counting filter is applied on the binary image to preserve only the high dense white pixel's areas and, morphological erosion-dilation is used to remove unnecessary small, thin white areas. Finally, remaining connected components of the binary image are used to crop candidate LP regions from contrast enhanced grayscale image. After the third stage, we have a number of candidate LP regions or images. In the fourth stage, firstly we use Bernsen binarization to convert a grayscale candidate LP region into a binary one. Then this binary candidate LP region is used to generate a binary perimeter version of the candidate LP region. At the end, we detect horizontal tilt angle from binary perimeter version of the candidate LP region and do necessary transformation to make it correct. In the fifth stage, we filter-out non-LPs from candidate LP regions based on LP's size, ratio, orientation, entropy and average counting. Remaining candidate LPs are the detected output LPs. Following subsections will give the detailed explanation for each of the stages.

### 3.2.1 Grayscale conversion, noise and rain effect removal

In the proposed ALPD, no color information is used as a feature for LP detection because color image processing is costly than grayscale image processing and color information is sensitive to uneven illumination. So the input color image should be converted into a grayscale image. The grayscale image may contain periodic (rain drops) and/or non-periodic noises, which creates unnecessary local irregularities within the image and decreases the performance of the ALPD. So noise removal is needed at the beginning

stage of the proposed ALPD method. The first stage consist of following 3 steps:

- RGB color image to grayscale conversion
- Rain effect removal
- Non-periodic noise removal

### 3.2.1.1 RGB Color Image to Grayscale Conversion

We use simple digital camera for taking car images. It provides RGB color image as input for the ALPD. Most often, a license plate have white characters on black background, or black characters on white background. In Bangladesh, most of the private-vehicle LPs are in this color format, and a few LPs have silver characters in black background. Even some of the commercial or government transports have LPs with black characters on green or yellow background, respectively. But this color variation is not important for the proposed ALPD because no color information is used as a feature for LP detection. The reason is that color information is highly sensitive to uneven illumination. So the proposed ALPD uses grayscale or binary image in every stage. Moreover, processing of a grayscale image is simpler than a color image and also grayscale image takes less space than a color image. To convert an RGB color image into a grayscale one, we use Equation (2.1). In Figure 3.2, we show an example of RGB color image with its grayscale image (G1) after conversion.



Figure 3.2: Conversion from (a) RGB color image to (b) grayscale image (G1).

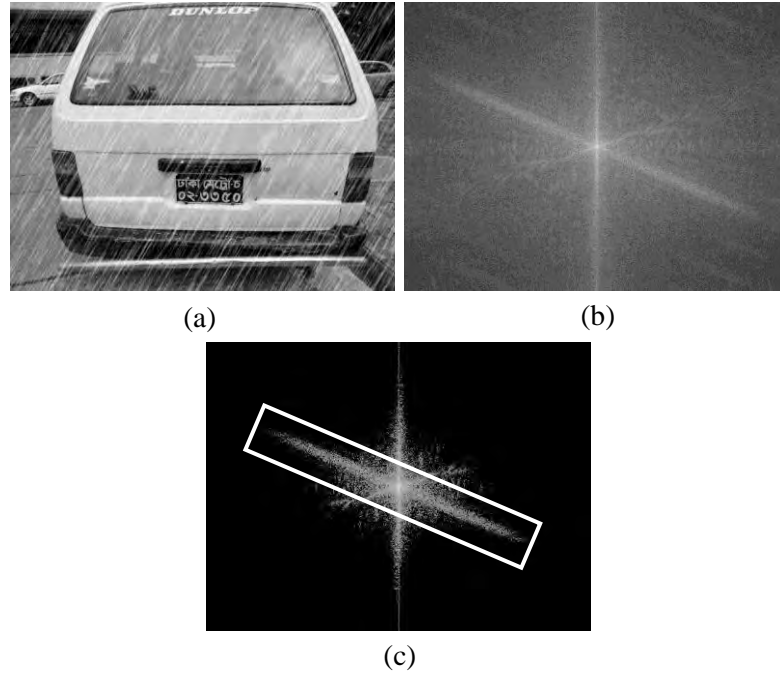


Figure 3.3: Example of (a) rain affected grayscale image (G1), (b) its Fourier image (F1) and (c) the thresholded Fourier image (F2).

### 3.2.1.2 Rain Effect Removal

During automatic detection of LP, presence of rain effect in the input image degrades the performance of the system. Presence of rain drops in the image creates unnecessary irregularities and increases number of candidate LP regions during ALPD. So removal or reduction of rain effect from the grayscale image (G1) is needed to improve the performance of the proposed ALPD. For removing rain drops from image, we consider rain as periodic noise. Periodic noise can be analyzed and filtered quite effectively in frequency domain. The basic idea is that periodic noise appears as concentrated burst of energy in the Fourier transformed image (see Section 2.2.3). Based on this basic idea, we develop an automatic rain removal technique which will effectively remove rain drops from image. First, we convert the rain affected grayscale image (G1) into Fourier image (F1) using DFT. In the Fourier image (F1), we scale all the frequency values within the range from 0 to 1. To preserve only the significant frequency values, we consider 0.5 as the threshold value. During thresholding, if any frequency value in the Fourier image (F1) is less than 0.5 then we replace it with zero. In Figure 3.3, we show an



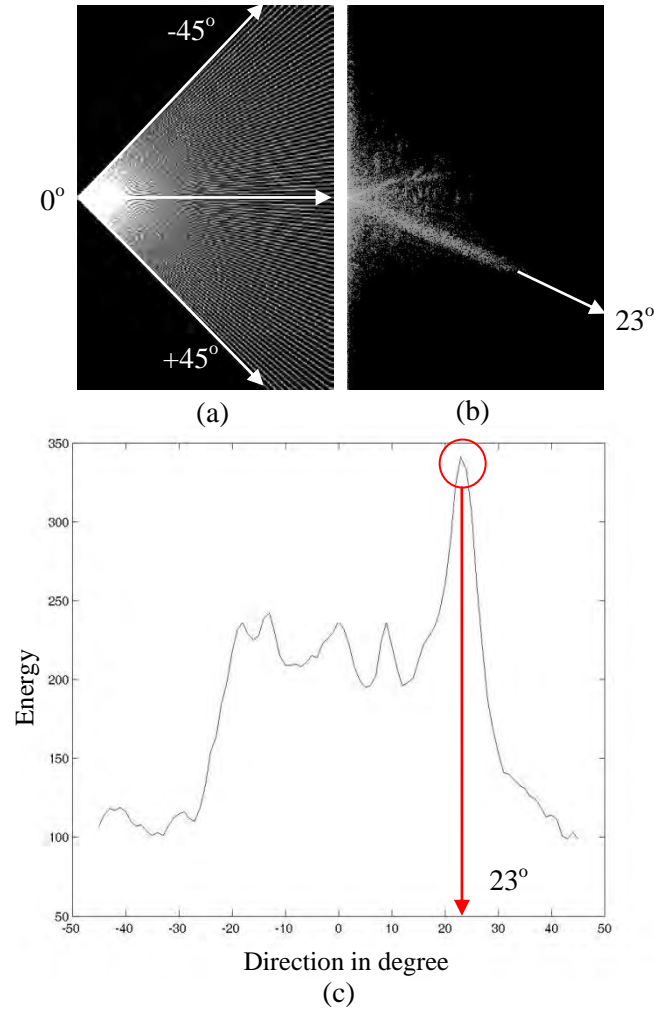


Figure 3.4: (a) The direction image, (b) an example of right half of the thresholded Fourier image (F2) and (c) the energy histogram for each direction.

example rain affected grayscale image (G1) with its Fourier image (F1) and also the thresholded Fourier image (F2). In thresholded Fourier image (F2), the white boxed portion is the energy burst due to rain noise. Experimentally we find that the direction of this energy burst is related to the direction of rain drops in the image. To locate the direction of rain energy in thresholded Fourier image (F2), we generate an energy histogram for each direction of energy. We have considered  $-45$  degree to  $+45$  degree as the range of direction for histogram. As we know that the thresholded Fourier image (F2) image is symmetric along the center vertical axis, so we take only the right half of the thresholded Fourier image (F2) during energy histogram computation. In Figure

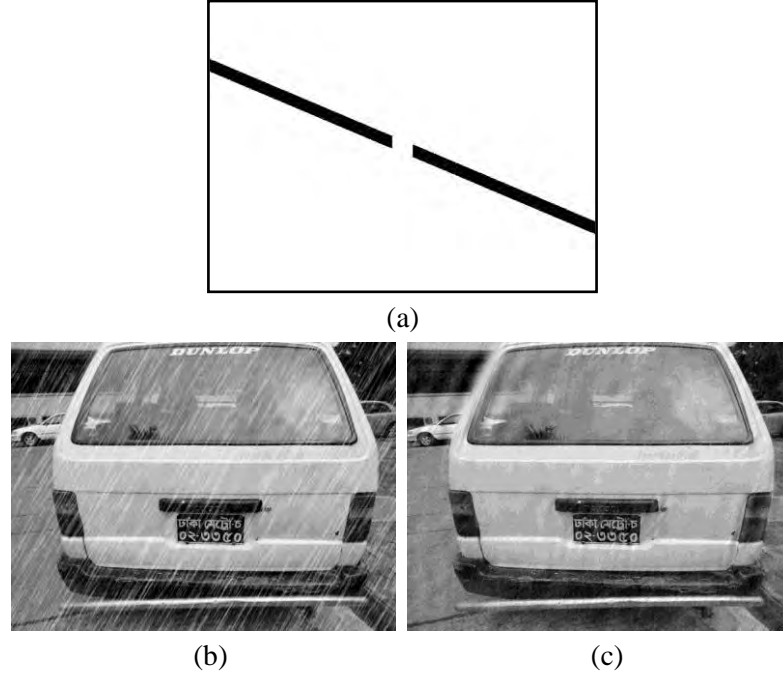


Figure 3.5: Example of (a) mask image, (b) an input rain affected grayscale image ( $G1$ ) and (c) the rain removed image ( $G1'$ ) after applying the mask.

3.4, the image (a) contains all the directions (as white lines) that we consider during energy histogram calculation, the image (b) is the example of half of the thresholded Fourier image ( $F2$ ) where the direction of the energy burst is 23 degree, and (c) is the energy histogram of half of the thresholded Fourier image ( $F2$ ) for direction -45 degree to +45 degree. From that energy histogram, the pick point gives the orientation information of the energy burst. Figure 3.4(c) shows the peak of the energy histogram which is pointing at 23 degree direction. After getting the orientation of the rain energy we automatically generate a rain mask in that direction and apply that mask on the Fourier image ( $F1$ ). This will remove the rain energy portion from the Fourier image ( $F1$ ). Finally, an inverse DFT of the Fourier image ( $F1$ ) gives the rain removed image ( $G1'$ ). An example mask image and a rain removed image ( $G1'$ ) is given in Figure 3.5.

### 3.2.1.3 Non-periodic Noise Removal

The ALPD method utilizes local irregularities (intensity transition) of an image as the initial LP localization feature, because irregularities inside LP region are high due to

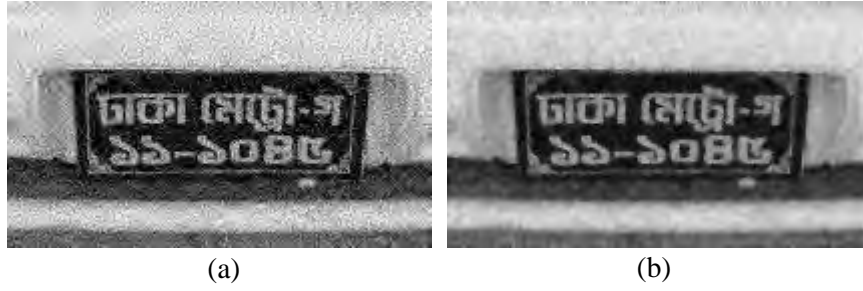


Figure 3.6: Example images (a) before and (b) after applying Wiener filter.

presence of text. But non-periodic noises (such as, small dirt, dust, surface textures) increase unnecessary irregularities in the image, which enhances number of non-LP regions at background. So for removing small noises, we use the local Wiener noise filter (see Section 2.2.12) of window size  $3 \times 3$  on grayscale image (G1) or rain removed image (G1') at this stage. We show an example of cropped LP image in Figure 3.6, where Wiener noise filter is applied on Figure 3.6(a) and gets the noise filtered image Figure 3.6(b). If we closely observe the Figure 3.6(a), then we see small white noises in the cropped LP image and they are removed or blurred after applying the noise filter. We apply the proposed ALPD without Wiener filter on the image dataset of 105 images (containing day light indoor and outdoor images) and find 472 candidate LP regions (105 original LP + 367 non-LP). But after applying the Wiener filter, we get 329 candidate LP regions (105 original LP + 224 non LP). That means Wiener noise filter at this stage helps subsequent stages of the ALPD by reducing number of unnecessary background elements. Furthermore, a noise filter needs to be applied before applying any contrast enhancement approach, because enhancement of image contrast also enhances the noise of that image. Therefore, the Wiener noise filter is used before going to second stage of the proposed ALPD. The use of Wiener filter gives few other benefits inside the ALPD system. There can be unnecessary boundary region around the detected LP due to presence of noise (or local irregularities). After using the Wiener noise filter, these boundary regions are minimized and gives acceptable areas of LP. Some comparative example images are given in Figure 3.7.

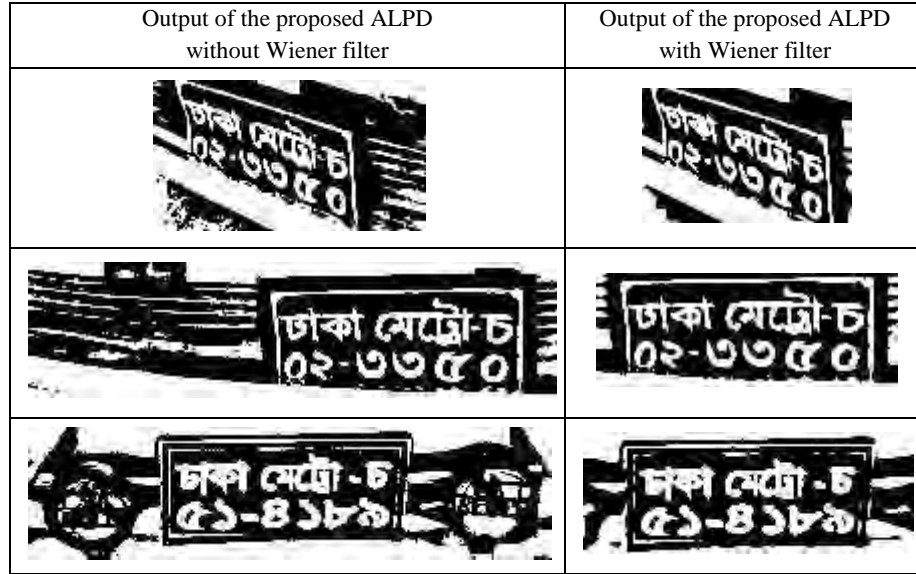


Figure 3.7: Example LP images showing the effect of using Wiener noise filter in the issue of extra boundary region.

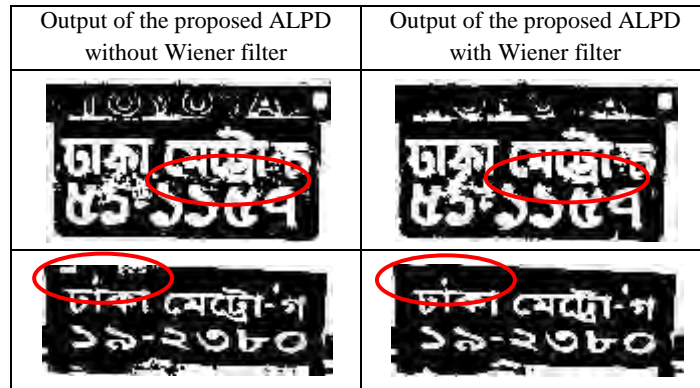


Figure 3.8: Example LP images showing the effect of using Wiener noise filter in the issue of Bernsen binarization.

In the third stage of the proposed ALPD, we use Bernsen binarization method which is sensitive to noise. That means noises will be more visible after Bernsen binarization. These unnecessary noise or white spots are not the part of LP feature and creates problem during filtering stage. In Figure 3.8, we show some comparative example images

where the effect of noise during binarization is reflected. If we observe the red circled area closely, then we see some small white spots (noise) inside LP region and, after using Wiener filter these noise are removed from the LP region.

### 3.2.2 Contrast Enhancement and Binarization

Hazardous conditions (such as, presence of fog and blur effects, low illuminated indoor and night environment) create lack of LP visibility within the image. So, contrast enhancement is necessary to improve the visibility of image contents. After contrast enhancement, the proposed ALPD uses local irregularities (standard deviation) as a feature for LP localization, because LP areas have significant local irregularities due to plate character's density and background. So at the second stage, the proposed ALPD has following 2 steps:

- Tamura-CLAHE contrast enhancement
- Standard deviation and mean based binarization

#### 3.2.2.1 Tamura-CLAHE Contrast Enhancement

An input image can be suffered from low contrast problem due to hazardous conditions (such as, night, indoor and blurriness). This problem degrades the performance of the ALPD in subsequent stages. The presence of fog effect in the input image also creates poor visibility or low contrast. We consider the fog removal problem as contrast enhancement problem. So we need to enhance the contrast of the noise removed image (G2) for successful detection of LP. But enhancing contrast without limit or without knowing the current contrast value of the image will lead to other problems such as, it can increase noise much, increase number of candidate LP regions and enlarge boundary regions of a detected LP. To enhance the contrast of an image in a reasonable way, we apply a new approach that uses the Tamura contrast value and the Contrast Limited Adaptive Histogram Equalization (CLAHE) jointly (see Section 2.2.5 and Section 2.2.9). Tamura contrast value  $F_{con}$  will give contrast value of an image within the range of 0 to 1. Higher value means high contrast image and lower value means low contrast image. To control the contrast limit  $C_{limit}$  of the CLAHE, we use Equation (3.1) where Tamura

value is subtracted from 1 and then divided by a constant  $div$ . Here,  $div$  is simply a divisor that control the range of  $C_{limit}$  values. Experimentally the value of  $div$  is set to 200 which gives  $C_{limit}$  values in the range from 0 to 0.005. Experimental analysis in Section (4.3) will justify this fact later.

$$C_{limit} = \frac{1 - F_{con}}{div} \quad (3.1)$$

This equation will generate the contrast limit in such a way that if an image have low contrast then the target contrast limit will be higher, and if an image have high contrast then the target contrast limit will be lower. When we use that contrast limit in CLAHE, it enhances the contrast of the noise removed image (G2) in a reasonable way and produces the contrast enhanced image (G3). Some example images after using the Tamura-CLAHE contrast enhancement are given in Figure 3.9. This new method also works well with the low contrast foggy image and thus improves the performance of LP detection. In Figure 3.10, we show a few examples of fog affected images, as well as, the improved versions after applying the Tamura-CLAHE enhancement.

### 3.2.2.2 Standard Deviation and Mean Based Binarization

In a grayscale image, LP areas have significant local irregularities due to plate character's density and background. That means occurrence of change of pixel-intensity is high in an LP area due to contrast between text and background. In the proposed ALPD, we apply a new binarization process that utilizes local irregularities as a feature for initial LP detection. This binarization process will segment out all the local irregularities (change of intensity) at dark side (where intensity value is low) in the form of high dense white pixel area.

In this binarization process, we convolve (see Section 2.2.2) a window of size  $S \times S$  over the contrast enhanced image (G3) for calculating local standard-deviation considering each pixel as the center of the window. This convolution step will give a standard deviation image (SD) having same size as the input image. Again, we convolve another window of size  $S \times S$  over the contrast enhanced image (G3) for calculating local mean. This will generate a mean image (M). Now apply pixel-wise comparison between mean

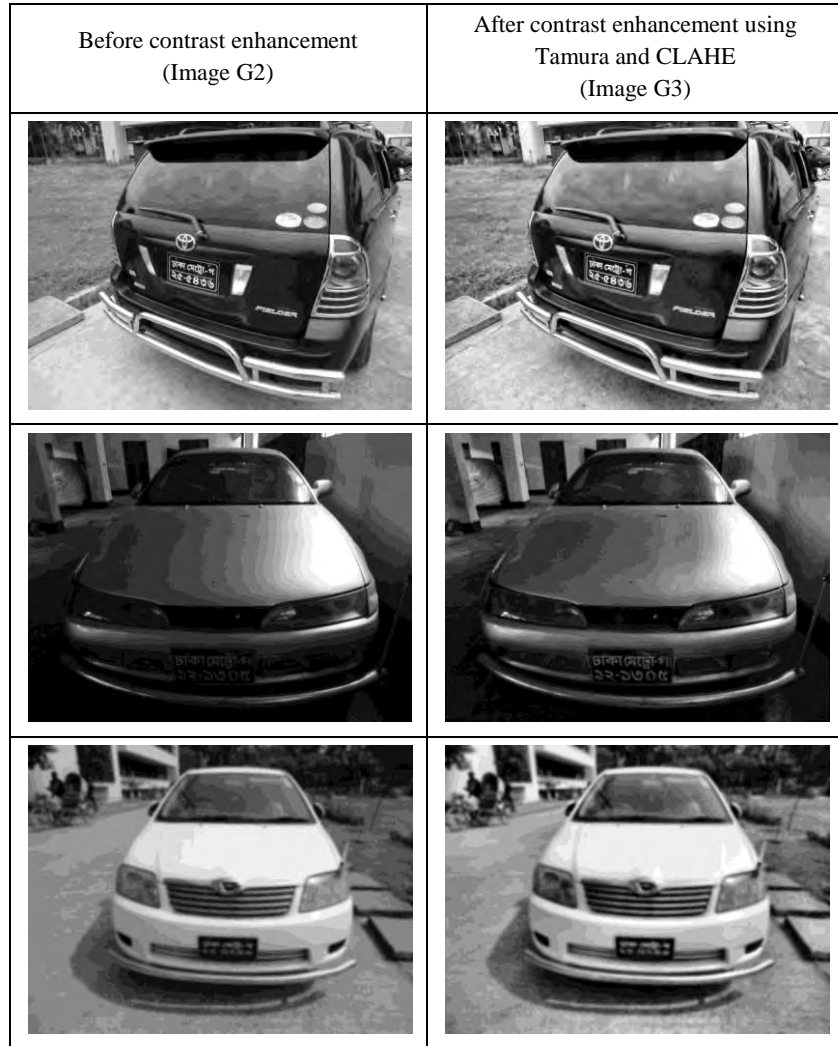


Figure 3.9: Example car images showing the effect of using Tamura-CLAHE contrast enhancement. The top image is in day-light condition, the middle one is in indoor condition and the bottom image contains blur effects.

image ( $M$ ) and standard deviation image ( $SD$ ), and produces a binary image ( $B1$ ) based on the following condition

$$B1(i, j) = \begin{cases} 1, & \text{if } SD(i, j) \geq k * M(i, j) \\ 0, & \text{else.} \end{cases} \quad (3.2)$$

where  $(i, j)$  is a pixel location and  $k$  is an experimentally determined parameter (see

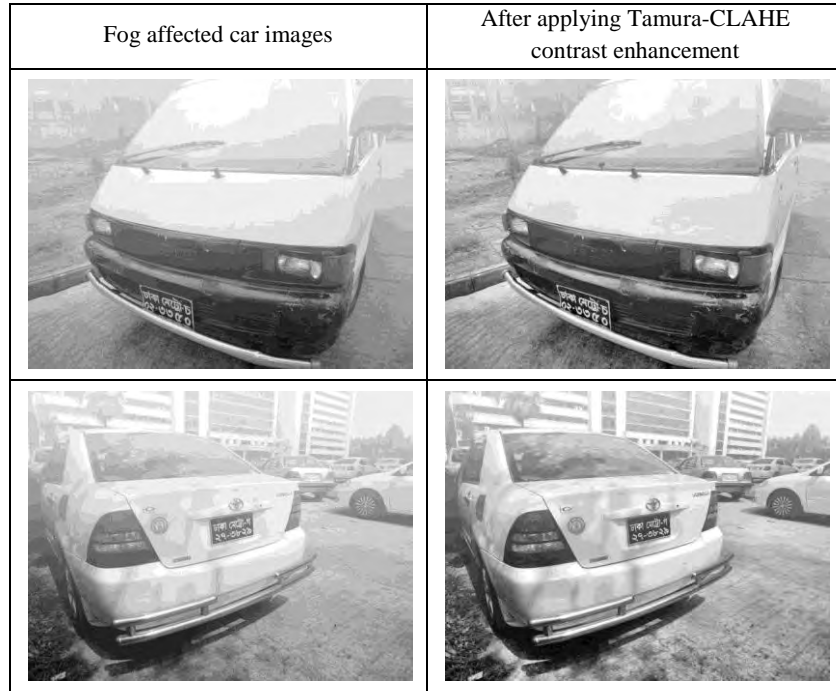


Figure 3.10: Performance of Tamura-CLAHE contrast enhancement over fog affected car images.

Section 4.4) in the range from 0 to 1. So far the best value of  $k$  for indoor-outdoor and rainy image is 0.3, for foggy and blurry image is 0.2, and for night image is 0.075. Figure 3.11 shows example mean image (M), standard deviation image (SD) and binary image (B1) for the same input car image.

In the equation (3.2), we make comparison between the standard deviation (2nd order) and the mean (1st order). The reason is that we want to satisfy the condition where the local standard deviation (change of intensity) is high but the local mean value (average intensity) is low. Due to this, in the binarized image (B1) it will make visible only those regions where values of pixel intensity is low (dark region) but the change of intensity is high in the grayscale image (G3). At the same time, it avoids regions where values of pixel intensity is high (bright region). In this way, it reduces white regions in the binarized image (minimizes the number of connected components). This process works well for LPs having black background with white characters, because mean values are low for black or near black background. If an image contains LP having



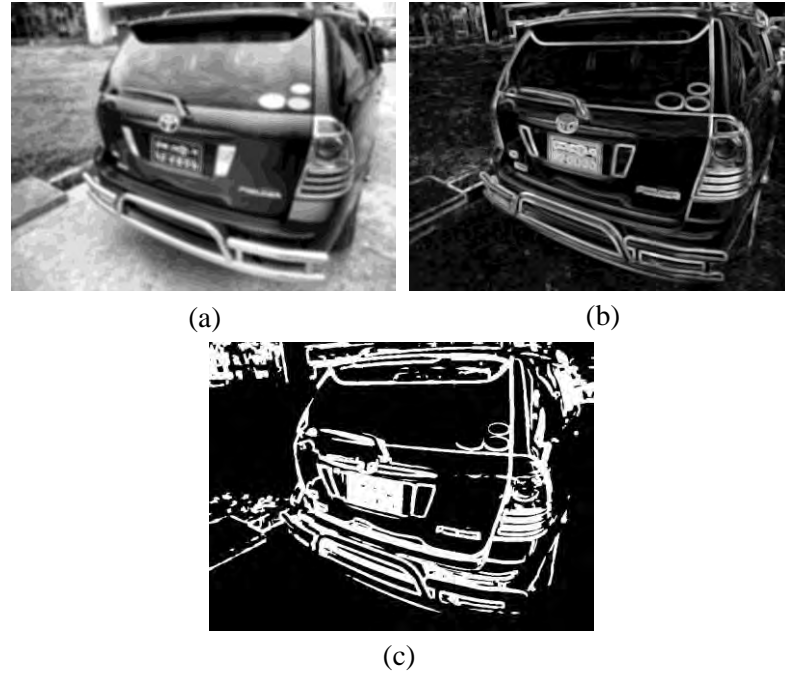


Figure 3.11: Examples of (a) mean image (M), (b) standard deviation image (SD) and (c) binary image (B1).

white background with black characters, then we need to take its negative image as the input for the binarization. In the equation (3.2), we also multiply the mean value with a factor  $k$ . The value of  $k$  ranges from 0 to 1. In this binarization process, a low value of  $k$  will decrease the mean value which means, it will satisfy the above condition for low standard-deviation value. On the other hand, high value of  $k$  will increase the mean value which means, it will satisfy the above condition for high standard-deviation value. Thus, for low contrast image environment we need to use lower value of  $k$ , and for high contrast image environment we need to use higher value of  $k$ .

If we closely observe the binary image (B1) then we see that it selects white pixels based on the amount of local irregularities (intensity transition). Amount of intensity transition inside an LP area is high, so this binarization process will give a high dense white-pixel area at LP region. Actually this binarization process will detect the boundary (change of color) and increase the width of the boundary of a high intensity area that is surrounded by low intensity area (like white characters on black LP background). To see the behavior of this binarization, we apply it on two simple artificially created

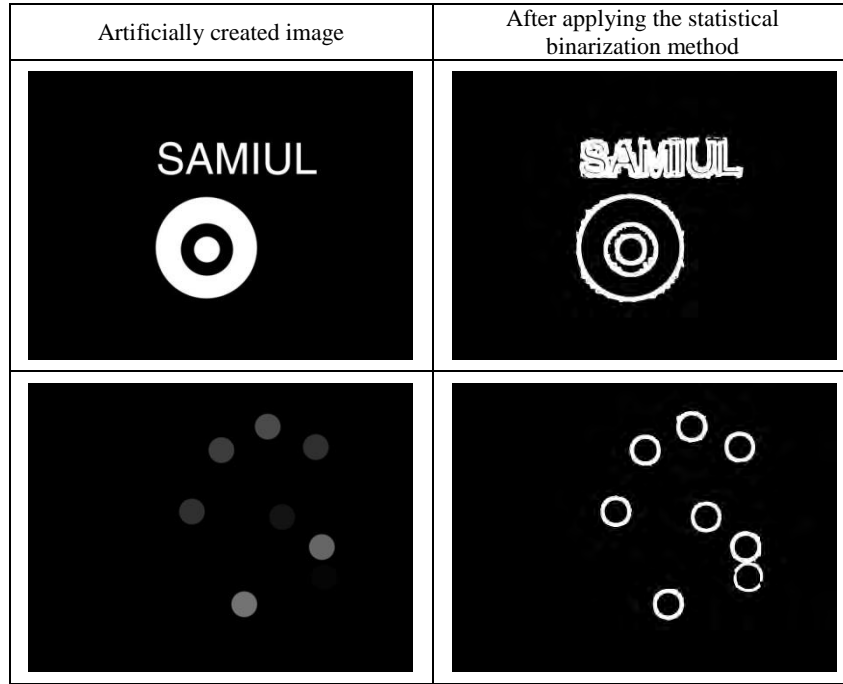


Figure 3.12: Artificially created images and their binarized version after applying the statistical binarization method.

images. Figure 3.12 shows these images before and after applying the binarization process. If we observe them closely then we will see that after applying the binarization process, it detects the boundary and increase the width of it. Here the boundary width depends on the size  $S$  of the window. Due to presence of character boundary in a LP, this binarization process will give high dense white pixel area in the output binary image (B1). Most of the LPs in Bangladesh are double lined and our image dataset contains images having average pixel distance of 7 between the two lines. So to connect these two lines during binarization, we use the window of size  $S = 7$ .

In the proposed ALPD, this second stage will solve all the low contrast problems like blur effect, low illuminated night effect, as well as, low contrast foggy environment and indoor image. Figure 3.13 shows some example noise removed images (G2) and their binarized version after applying the second stage. We use this binary image (B1) in the next stage for detecting LP area from the input image.



Figure 3.13: Contrast enhanced images (G2) and their binary images (B1) after applying the second stage. The top image is affected by fog, the middle one has low illuminated night effect and the bottom image contains blur effect.

### 3.2.3 Local Counting Filter and CCC

After the second stage, the binary image (B1) contains high dense white areas at the same place where the change of intensity value is high in the input image. As we know that the change of intensity is high within an LP area (due to LP text and background), so we need to preserve all the high dense white areas of the binary image (B1). Before going to connected component analysis, we have to fill small holes and remove small

thin white areas from the binary image (B1). To do these, the proposed ALPD have following steps at the third stage:

- Local counting filter
- Morphological erosion and dilation
- Cropping connected components

### 3.2.3.1 Local Counting Filter

At the beginning of third stage, we apply local counting filter that preserves high dense white areas, as well as, fill small holes of binary image (B1). Here, a window of size  $S \times S$  is convolved over the binary image (B1) and counts number of 1's (white pixels) in that window. If majority (more than 50 percent) pixels of that local window contain 1's pixels, then put a 1 in the center pixel position, otherwise 0. After this convolution, we get a filtered binary image (B2). In this counting filter, the size of the window is half of the average license plate height, because the binary image (B1) contains high dense white area in the place of an LP area (due to text boundary). Our image dataset contains images having average LP height of 40 pixels, so the window size  $S$  is 20. Example of an filtered binary image (B2) is given in Figure 3.14(b).

### 3.2.3.2 Morphological Erosion and Dilation

Before cropping connected components (CCC), we have to remove small thin white areas, unnecessary boundary regions of an LP and thin connectivity between large white objects. To do so, we use morphological erosion followed by dilation on filtered binary image (B2) using a disk as structuring element (see Section 2.2.10). The radius of the disk depends on the size of the LP area. So during experiment we use a disk of radius 20 (half of average height of LP) pixels for erosion and dilation. Example of an dialated binary image (B3) is given in Figure 3.14(c).

### 3.2.3.3 Cropping Connected Components

From the dialated binary image (B3) we label all the binary connected components (see Section 2.2.8) based on 8-neighboring connectivity. The dialated binary image (B3)

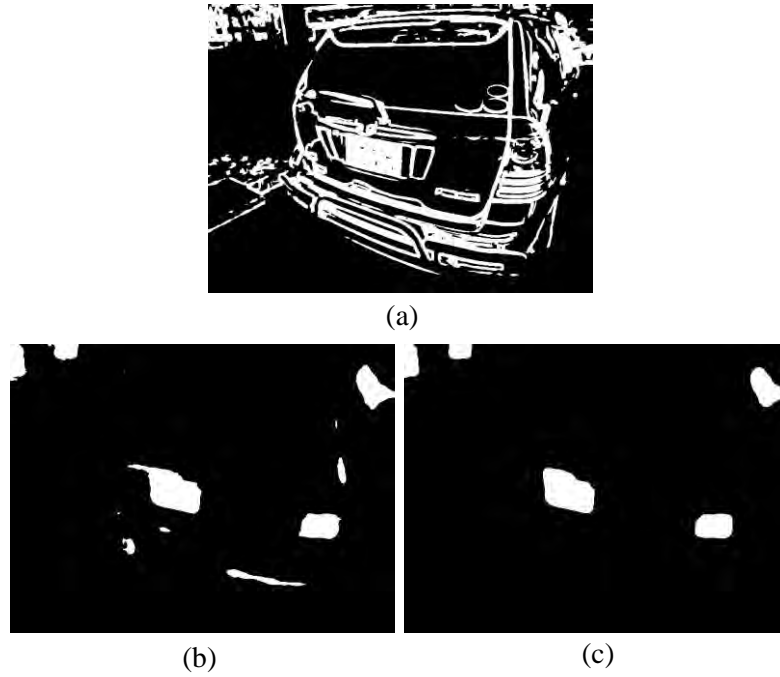


Figure 3.14: Example of (a) binary image (B1), (b) filtered binary image (B2) and (c) dialated binary image (B3).

contains number of connected components. Figure 3.15(a) shows an example of dialated binary image (B3) with all its lebeled components (suppose  $C_1, C_2, C_3, C_4 \dots$  and so on). Based on the component's region, we make rectangular cropping from the contrast enhanced image (G3). After that cropping, we have number of candidate LP regions. Figure 3.15(b) shows all the cropped rectangular areas (white boxes, suppose  $LP_1, LP_2, LP_3, LP_4 \dots$  and so on) from contrast enhanced image (G3). Among those candidate LP regions, one of them is the actual LP and others are not. A good quality filtering or analysis is needed in the next stages for finding the actual LP area.

### 3.2.4 Tilt Angle Detection and Correction

In the proposed ALPD, we also consider the issue of horizontally tilted LP. A license plate image can be horizontally tilted due to camera position and angle. Our new tilt correction method detects the horizontal tilt angle in the range from 0 degree to 30 degree (for both left and right tilt), as well as, make necessary transformation for the

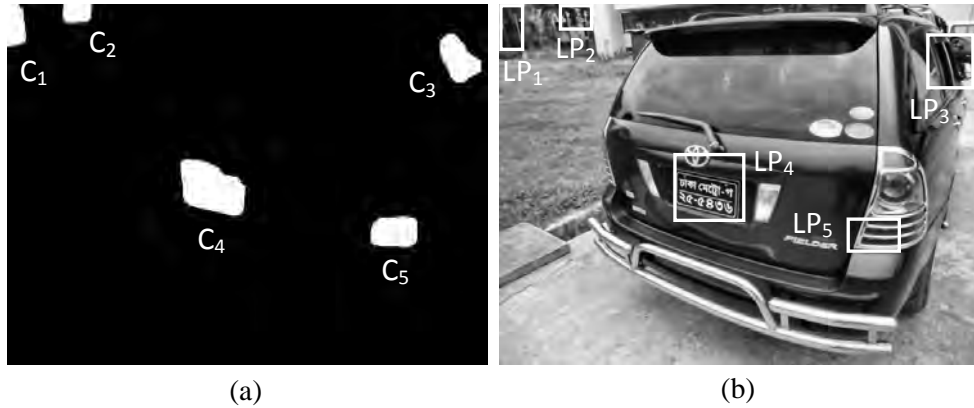


Figure 3.15: Example of (a) dialated binary image (B3) with labeled components and (b) cropped candidate LP regions from contrast enhanced image (G3).

correction. For this purpose, the proposed ALPD has following 2 steps in the fourth stage:

- Bernsen binarization and binary perimeter version of candidate LP
- Radon transform based tilt angle detection and correction

#### 3.2.4.1 Bernsen Binarization and Binary Perimeter Version of Candidate LP

At first, for tilt angle detection, we use the binary perimeter image (see Section 2.2.7) of the cropped candidate LP region. Because grayscale intensity information is not necessary for detecting tilt angle, only the boundary or edge information in binary format is sufficient. To do so, we apply the Bernsen binarization method (see Section 2.2.6) on the grayscale candidate LP images or regions ( $LP_1$ ,  $LP_2$ ,  $LP_3$ ,  $LP_4$  . . and so on), and then generate the boundary or perimeter image from the Bernsen binary image. We use Bernsen as an intermediate binarization method because it works well even in the irregular illumination condition, such as, exposure and shadow. Few example candidate LP images are shown in Figure 3.16 along with Bernsen binarized and binary perimeter versions.

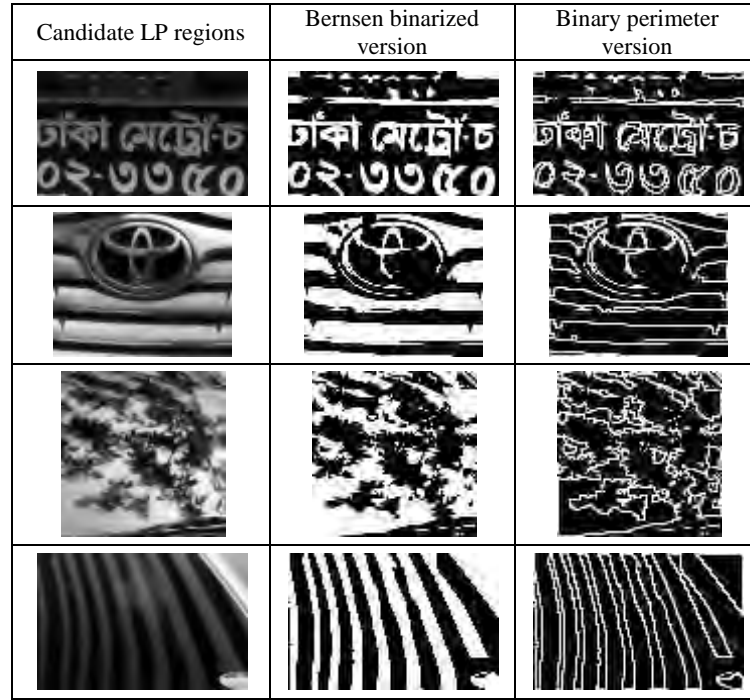


Figure 3.16: Example images of candidate LPs with their Bernsen binarized and binary perimeter version.

#### 3.2.4.2 Radon Transform Based Tilt Angle Detection and Correction

Due to highly dense text boundary on LP, directional information of the text on the LP will give the angle information of the tilted LP. To detect the directional information of the LP text, we apply Radon transformation (see Section 2.2.11) from  $-90$  degree to  $+90$  degree on the binary perimeter image and obtain the transformed image. In the transformed image or matrix, all the bright spots will provide dominant directional information. There are total 181 columns (from 0 degree to 180 degree) in the transformed image where  $n$ th column means degree  $n$ . So the column value of a bright spot will give the directional information. To find the highest dominant direction, this transformed image is binarized based on near maximum intensity values. From that binarized transformed image, we take the average column values of white pixels (binary 1) as the tilt angle. Figure 3.17 shows a few examples of perimeter images of LP with their Radon transformed and binarized Radon transformed image. In that Figure, a downward red

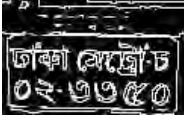
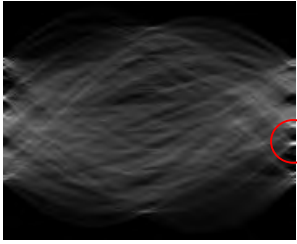

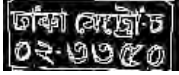

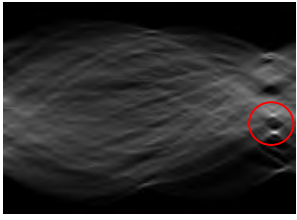



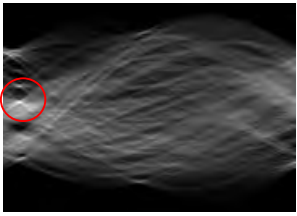


Binary perimeter Image	Radon transformed image	Binarized Radon transformed image	After tilt correction
			
			
			

Figure 3.17: Images showing steps of tilt detection and the output candidate LP regions after tilt correction.

arrow is pointing the value of detected tilt angle on the binarized Radon transformed image. After detecting the tilt angle, we apply affine transformation based on detected angle to make the candidate LP region straight. Also we crop unnecessary upper and lower margin of corrected LP region based on the amount of white pixel density at margin area. Images of a few tilt corrected LP regions are shown in Figure 3.17. The major advantage of Radon transform based tilt detection is that due to use of projection information (see Section 2.2.11), the dominant direction is not sensitive to small noises or character connectivity of LP text.

### 3.2.5 Filtering Non-LP Regions

After the end of first four stages, we have number of tilt corrected candidate LP regions. But among those candidate LP regions one of them is the original LP region and others





Figure 3.18: Examples of candidate LP images that are rejected as non-LP due to undersized resolution.

are non-LPs. In this last stage, we filter-out all the non-LP regions from the candidate LP set based on few basic LP features such as, LP size, aspect ratio, orientation, entropy and average counting of horizontal white pixels. For this purpose, the proposed ALPD has following 3 steps in the last (fifth) stage:

- Filtering non-LP regions based on size, ratio and orientation
- Filtering non-LP regions based on entropy
- Filtering non-LP regions based on average counting

### 3.2.5.1 Filtering Non-LP Regions Based on Size, Ratio and Orientation

At first, we filter-out non-LP images based on the LP resolution or size in the captured image. For fixed-distance image capturing, resolution of LP text region is more or less equal for different car images, because practically a license plate should follow a standard size during production. Our experimental images (resolution 640 by 480) are taken from approximately 1.0 to 1.5 meter distance where average resolution of non-tilted LP is 120 by 40 and tilted LP is 80 by 55. Even the minimum width and height are 62 and 31 pixels, respectively. Based on this experimental data, we reject those candidate LPs that are small in size having width less than 30 pixels or height less than 60 pixels. Some example images of rejected candidate LPs are given in Figure 3.18.

For filtering non-LP regions, we also use the width-height ratio as a feature. Almost every LP regions are horizontally elongated rather than vertically. Even tilted LP regions are not vertically elongated. Experimentally we find that candidate LP regions having aspect ratio less than 0.9 are not the target LP regions. So we reject these candidate LP regions as non-LP. Figure 3.19 shows a few examples of candidate LP regions that are rejected due to unsatisfied width-height ratio.

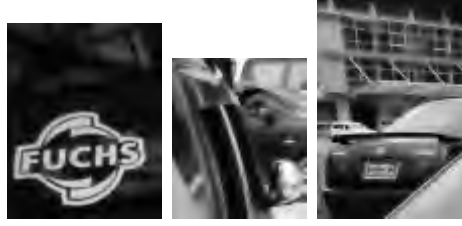


Figure 3.19: Examples of candidate LP images that are rejected as non-LP due to unsatisfied width-height ratio.



Figure 3.20: Examples of candidate LP images that are rejected as non-LP due to unconvinced orientation angle.

In the fourth stage of our ALPD, we already detect the dominant orientation angle of the candidate LP regions within the range from 0 degree to 180 degree. But to involve the orientation angle as filtering feature, we allow maximum 30 degree tilt angle for both left and right tilted LP. In the Radon-transformed candidate LP image, left tilt angle is detected within 1 degree to 30 degree and right tilt angle is detected within 150 degree to 179 degree. Zero tilted candidate LP regions gives 0 degree or 180 degree angle in the binarized Radon transformed image. So any candidate LP region having dominant orientation angle within the range of 31 degree to 149 degree is rejected as non-LP region. Some example candidate LP images are given in Figure 3.20, that are rejected as non-LP due to dominant pixel orientation.

### 3.2.5.2 Filtering Non-LP Regions Based on Entropy

For filtering non-LP images, we introduce a new approach which is based on entropy (amount of information) measure. Before calculating the entropy value, we apply a local vertical counting filter of size  $3 \times 1$  on the binary perimeter version of the candidate LP

image. Then we binarize the binary perimeter image based on the vertical-counting value in such way that if a local counted value is 3 then consider a 1, otherwise 0. Let, denotes this binary candidate LP image as  $LP_{ver}$ . The intuition is that license plate has high density or amount of vertical edges due to characters and alphabets. So after applying the counting filter and binarization, the candidate LP image ( $LP_{ver}$ ) have high chance to have many vertical white points than others. During filtering, we chose entropy (see Section 2.2.4) as the measure of amount of information in bit/pixel. For binary image, maximum value of entropy is 1 bit/pixel. Experimentally we find that, if the entropy value is less than 0.2 then we can filter the binary candidate LP image ( $LP_{ver}$ ) as non-LP. Figure 3.21 shows a few candidate LP images (in perimeter version) and the output image ( $LP_{ver}$ ) after applying the local vertical counting filter and binarization. Some of the candidate LP regions are rejected as non-LP due to unconvinced entropy value.

### 3.2.5.3 Filtering Non-LP Regions Based on Average Counting

The non-LP regions that survive in the previous stage can be completely filtered using average counting. So, for more filtering, we counts the number of 1's for each row of the binary candidate LP image ( $LP_{ver}$ ) and calculate the average counting. Experimentally we find that if the average counting per row is less than 3.5 then we can filter it as non-LP. Examples of candidate LP images are given in Figure 3.22 that are rejected after average counting of horizontal white pixels. After filtering non-LPs, the rest of the candidate LPs are considered as detected LP regions.

## 3.3 Conclusion

In this chapter, a new ALPD method is described that has the ability to handle hazardous conditions. This ALPD method comprises of five stages. In the first stage, the input RGB color image is converted to a grayscale image. To handle rain affected input image, a novel rain removal technique is used in this stage. Then a well-known Weiner noise filter is also applied on the grayscale image to remove small noise. In the next stage, to solve the problem of low contrast image (such as, indoor, blurry, night and foggy image), a new Tamura-CLAHE contrast enhancement method is applied. Then





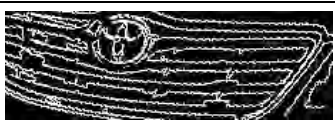







Binary perimeter version of candidate LP image	After applying local vertical counting filter and binarization ( $LP_{ver}$ )	Rejected or accepted
		Rejected
		Rejected
		Rejected
		Accepted
		Accepted
		Accepted

Figure 3.21: Examples of candidate LP images and the output images after applying vertical counting filter. Entropy based filtering decisions are also reflected at the rightmost column of the Figure.

the contrast enhanced image is binarized based on local statistical data of the image. This novel statistical binarization method has the ability to give visibility of very low contrast area in binary format. At third stage, the binary image is processed by using a new local counting filter and traditional morphological operation. Then all the connected components are segmented from the processed binary image. These cropped components are the candidate LP regions for the next stages. To detect tilt angle of a candidate LP region, an innovative approach based on Radon transformation is used at the fourth stage. Finally, non-LP regions are rejected from the candidate LP set based on LP size, aspect ratio, orientation and average horizontal counting. In addition, a novel entropy based filtering technique is also applied at the end to filter-out the remaining non-LPs. After filtering, the rest of the candidate LPs are the desired original







Binary perimeter version of candidate LP image	After applying local vertical counting filter and binarization ( $LP_{ver}$ )	Rejected or accepted
		Rejected
		Rejected
		Rejected

Figure 3.22: Examples of candidate LP images that are rejected after applying average horizontal counting. Filtering decisions are also reflected at the rightmost column of the Figure.

LP. In the next Chapter, the performance of the proposed ALPD is evaluated using different types of image dataset. Furthermore, we also compare the proposed ALPD with two existing state-of-the-art ALPD techniques.

## Chapter 4

# Experimental Studies

### 4.1 Introduction

In Chapter 3, we propose a new ALPD system to detect LPs from image with new approaches for rain removing, contrast enhancement, binarization, tilt correction and filtering non-LPs. In this Chapter, the proposed ALPD is implemented using MATLAB 7.12 on a personal computer equipped with Intel Core 2 Duo CPU T6600 at 2.2 GHz processor and 2 GB RAM. The implemented ALPD is applied on 525 car images [3] having different hazardous conditions (night, indoor, blurry, foggy, rainy), as well as, normal day-light condition. Moreover, we test the ALPD on 325 car images containing English license plates taken from an online license plate database [4]. We also implement the ALPD systems presented in [6, 7] using MATLAB 7.12 and compare them with the proposed ALPD. Experimental analysis for selecting the best possible value of few parameters ( $div$  and  $k$ ) are also given in this Chapter.

### 4.2 Image Database and Performance Measurement

For experimental purpose, we create an image database [3] that contains 525 car images having potential LP written in Bangla. Images are taken using a simple digital camera and the spatial resolution of the images are  $640 \times 480$ . In this Bangla LP database, out of 525 images 225 of them are rain affected. Among those, 105 images have heavy rain effects with  $-45$ ,  $-30$ ,  $-15$ ,  $0$ ,  $+15$ ,  $+30$  and  $+45$  degree rain streak's orientations, 60 im-

Table 4.1: Summary of the rain-affected car image dataset (total 225 images).

Level of rain effects	Rain orientation	No. of images
Heavy	-45 degree	15
	-30 degree	15
	-15 degree	15
	0 degree	15
	+15 degree	15
	+30 degree	15
	+45 degree	15
Moderate	-45 degree	15
	-30 degree	15
	-15 degree	15
	0 degree	15
Light	-30 degree	15
	-15 degree	15
	+15 degree	15
	+30 degree	15

Table 4.2: Summary of the non-rain image dataset (300 car images having normal and hazardous conditions).

Condition	No. of images
Normal (Day-light)	100
Fog affected	80
Blur	40
Indoor	40
Night	40

ages have moderate rain effects with -45, -30, -15 and 0 degree rain streak's orientations, and rest of the 60 images have light rain effects with +30, -30, +15 and -15 degree rain streak's orientations. Summary of the rain affected image dataset is given in Table 4.1. Figure 4.1 shows some sample rain-affected car images from that image database.

In the database [3], the rest of 300 car images are not affected by rain, but it contains images having different hazardous conditions, as well as, simple day-light images. Among 300 images, 100 images have day-light environment, 40 images have indoor environment, 80 images have foggy condition, 40 images have blurry condition and remaining 40 images have night environment. Summary of the non-rain image dataset is given in Table 4.2. Figure 4.2 shows some sample non-rain car images from that image database. Moreover, among these 525 car images, 175 images have left tilted LP, 175 images have

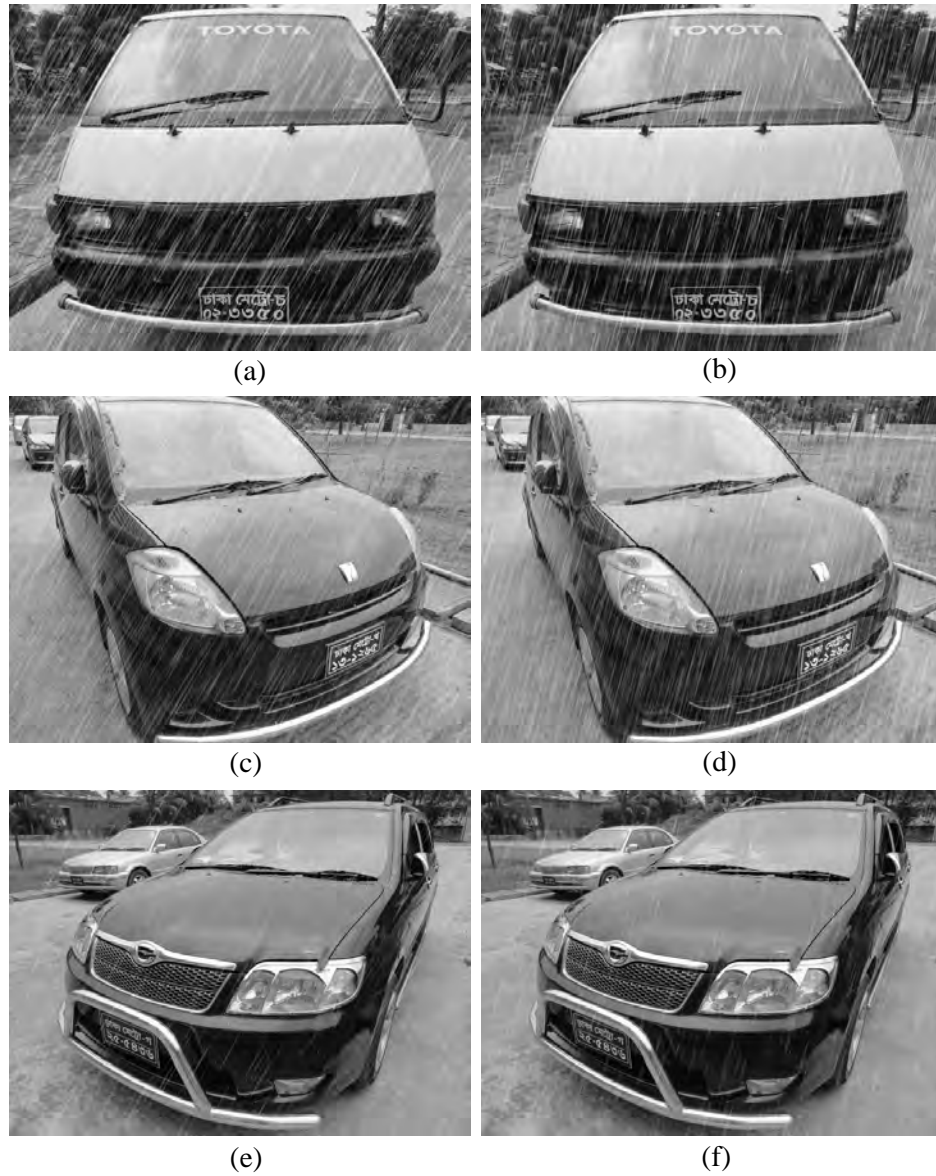


Figure 4.1: Examples of rain affected car images from the Bangla LP database [3]. Heavy-rain affected images with (a) -30 degree rain orientation and (b) -15 rain orientation. Moderate rain-affected images with (c) -30 degree rain orientation and (d) -15 rain orientation. Light rain-affected images with (e) -30 degree rain orientation and (f) -15 rain orientation.

right tilted LP and rest of the images have LP with no tilted condition.

During the experiment, we use another online image database [4] that contains 325 car images having LP written in English. These images have left tilted, right tilted and straight LPs, have different types and colors of LPs, have night, indoor, day-light and



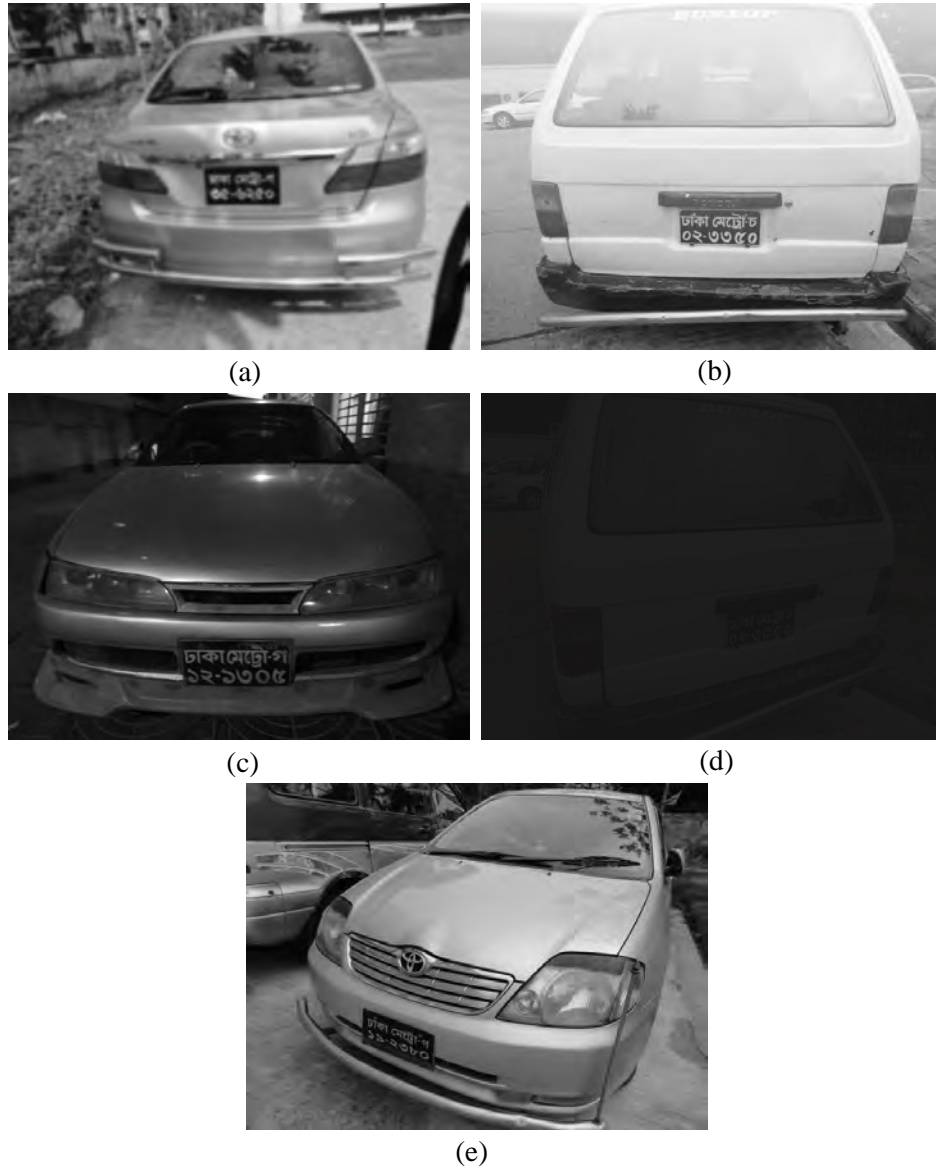


Figure 4.2: Examples of non-rain car images from the Bangla LP database [3]. (a) blurry, (b) foggy, (c) indoor (d) night and (e) day-light conditions.

uneven illumination conditions. But the database does not contain any images having rain, fog and blur effects. Figure 4.3 shows some sample car images from the English LP image database.

For performance measure, we use detection rate as the performance metric. Detection rate depends on the number of input car images and the number of detected LP regions after applying any ALPD method. Here, each input car image must contain ex-

actly one potential LP region. The Equation for finding the detection rate is given below.

$$\text{Detection rate} = \frac{\text{Number of original LP regions in filtered LP set}}{\text{Number of target LP regions in the input image set}} \times 100\%. \quad (4.1)$$

We also consider the average running time of the ALPD methods as the performance metric. Average running time means average processing time of an ALPD method to detect potential LP regions from an input image. It depends on the total time taken by the ALPD to process input images and the number of input images. The Equation for finding the average running time is given below.

$$\text{Average running time} = \frac{\text{Total time taken by the ALPD to process input images}}{\text{Number of input images}}. \quad (4.2)$$

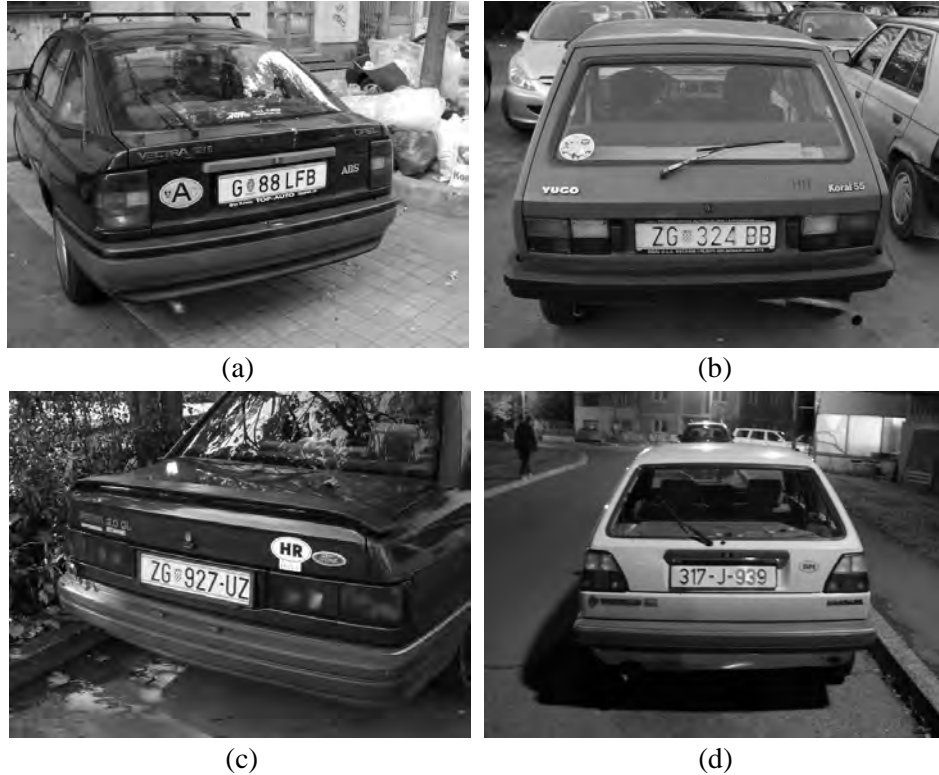


Figure 4.3: Examples of car images from the English LP database [4]. (a) left tilted, (b) straight LP, (c) right tilted and (d) night conditions.

### 4.3 Experimental Analysis on the Value of $div$

In the proposed ALPD, we use a new approach (Tamura-CLAHE contrast enhancement) for enhancing contrast of an image in a balanced way (see Section 3.2.2.1). In the Equation (3.1), Tamura value  $F_{con}$  is subtracted from 1 and then divided by a divisor  $div$ . This equation will generate the contrast limit  $C_{limit}$  of the CLAHE in such a way that, if an image have low contrast then the target contrast limit will be higher, and if an image have high contrast then the target contrast limit will be lower. In Equation (3.1), the divisor  $div$  is used to control the range of  $C_{limit}$ . The value of  $div$  is decided based on the experimental results of the proposed ALPD. We applied the proposed ALPD on 200 non-rain car images from Bangla LP database [3] for different value of  $div$ . The experimental results are given in Table 4.3. In the Table, the detection rate is calculated using the Equation (4.1).

Table 4.3: Performance of the proposed ALPD for different values of  $div$ .

$div$ values	No. of detected LPs (out of 200 images)	Detection rate (%)
1	124	62.00
100	173	86.50
200	177	88.50
300	169	84.50
400	159	79.50
500	157	78.50
600	152	76.00
No enhancement	127	63.50

In the Table 4.3, you can see that when no contrast enhancement is applied inside the ALPD, then the detection rate is only 63.50%. But when Tamura-CLAHE contrast enhancement with  $div$  value 200 is used inside the ALPD, then the increased detection rate is 88.50%. In the Equation (3.1), increasing the value of  $div$  will decrease the value of  $C_{limit}$ . When the value of  $div$  is 1, then the value of  $C_{limit}$  is maximum. But over-enhancement increases the noise highly and as a consequence detection rate drops. In the Table 4.3, the maximum value of  $div$  is 600 which also decrease the performance of the ALPD due to insufficient value of  $C_{limit}$ . Experimentally, the best value for  $div$  is 200.

#### 4.4 Experimental Analysis on the Value of $k$

In the proposed ALPD, we use a new binarization method (standard deviation and mean based) to convert the grayscale image into a binary one (see Section 3.2.2.2). During binarization, we use the conditional Equation (3.2), where  $k$  is a factor in the range from 0 to 1. In this binarization process, low value of  $k$  means it will satisfy the condition for low standard-deviation value. On the other hand high value of  $k$  means it will satisfy the condition for high standard-deviation value. Thus for low contrast image environment we need to use lower value of  $k$ , and for high contrast image environment we need to use higher value of  $k$ . There was no evidence that there is a best possible way to choose a value for  $k$ . This is to be decided according to the experimental performance (detection rate) of the proposed ALPD for different values of  $k$ . Table 4.4, 4.5, 4.6, 4.7 and 4.8 show the experimental results of the proposed ALPD for different values of  $k$  at different conditions (day-light, indoor, fog, blur and night). From the Table 4.4 and 4.5, the best value of  $k$  for day-light and indoor image is 0.300. From the Table 4.6 and 4.7, the best value of  $k$  for foggy and blurry image is 0.200. Although for blurry images, both  $k = 0.150$  and  $k = 0.200$  shows same level of detection rate (75.00%), but binarization with  $k = 0.200$  produces less number of candidate LP regions. So, the value of  $k = 0.200$  is selected for blurry images. From the Table 4.8, the best value of  $k$  for night image is 0.075.

Table 4.4: Performance of the proposed ALPD for day-light car images at different values of  $k$ .

$k$ values	No. of detected LPs (out of 80 images)	Detection rate (%)
0.200	65	81.25
0.250	72	90.00
0.300	76	95.00
0.350	70	87.50
0.400	65	81.25

Table 4.5: Performance of the proposed ALPD for indoor car images at different values of  $k$ .

$k$ values	No. of detected LPs (out of 40 images)	Detection rate (%)
0.200	27	67.50
0.250	35	87.50
0.300	39	97.50
0.350	34	85.00
0.400	30	75.00

Table 4.6: Performance of the proposed ALPD for foggy car images at different values of  $k$ .

$k$ values	No. of detected LPs (out of 80 images)	Detection rate (%)
0.100	50	62.50
0.150	57	71.25
0.200	65	81.25
0.250	55	68.75
0.300	41	51.25

Table 4.7: Performance of the proposed ALPD for blurry car images at different values of  $k$ .

$k$ values	No. of detected LPs (out of 40 images)	Detection rate (%)
0.100	25	62.50
0.150	30	75.00
0.200	30	75.00
0.250	18	45.00
0.300	5	12.50

Table 4.8: Performance of the proposed ALPD for night's car images at different values of  $k$ .

$k$ values	No. of detected LPs (out of 40 images)	Detection rate (%)
0.025	15	37.50
0.050	25	61.50
0.075	33	82.50
0.100	20	50.00
0.125	13	32.50

## 4.5 Experimental Analysis on Average Counting Value

At the fifth stage of the proposed ALPD, we use average horizontal counting as the condition for filtering non-LPs. We apply a threshold value of average counting for re-

Table 4.9: Number of misselections for different threshold values of average counting.

Different threshold values of average counting	No. of true rejection	No. of false acceptance
2.0	0	37
2.5	0	23
3.0	0	18
3.5	0	13
4.0	1	13
4.5	7	10
5.0	10	8
5.5	24	8
6.0	34	5

jecting a candidate LP region as non-LP. Due to hazardous conditions, it is impossible to set a threshold value intuitively. So, experimentally we set a threshold value of average counting in which the filtering approach shows minimum number of misselections. Here misselection means, rejection of a potential LP as non-LP (true rejection) and acceptance of a non-LP as potential LP (false acceptance). For this experiment, we use 507 automatically detected candidate LP regions (450 potential LPs + 57 non-LPs). we apply the filtering approach separately on these candidate LP regions for different threshold values of average counting (ranges from 2.0 to 6.0). Table 4.9 shows the number of misselections for different threshold values of average counting. In the table, for the value of 3.5 the number of misselection is minimum. Increasing the threshold value also increase the number of misselections. So the best threshold value of average counting is 3.5.

## 4.6 Experiment on Rain-affected Images

In the previous chapter, we present a new rain removal technique for the proposed ALPD. It detects the rain streak's orientation in the frequency domain and then removes rain frequencies from the input image using automatically generated rain mask. To test our rain removal technique, we take the 225 rain affected car images from Bangla LP database [3] and apply the new rain removal technique on these rain-affected car images. The new rain removal technique successfully removes rain effects from all 225 images.

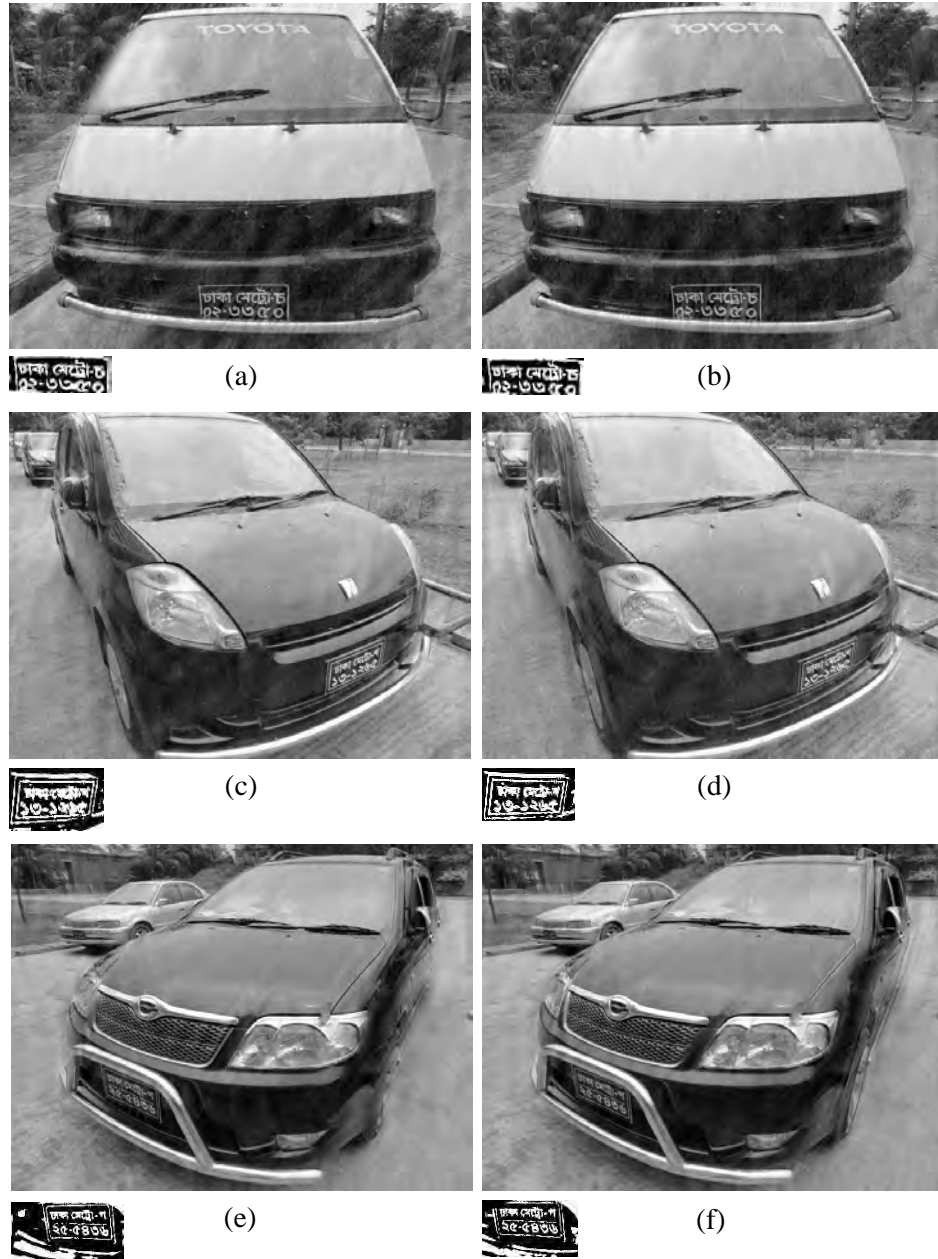


Figure 4.4: Rain-removed versions (a)-(f) after applying the proposed rain removal technique on the images of Figure 4.1(a)-(f). Detected LP regions (by the proposed ALPD) are also given just below the individual image.

The average running time for the new rain removal approach is 0.73 seconds. Figure 4.4 shows the rain-removed version of the images of Figure 4.1.

We also compare our rain removal technique with an existing rain removal approach [5]. In [5], it uses bilateral filter to decompose the input image into high frequency and

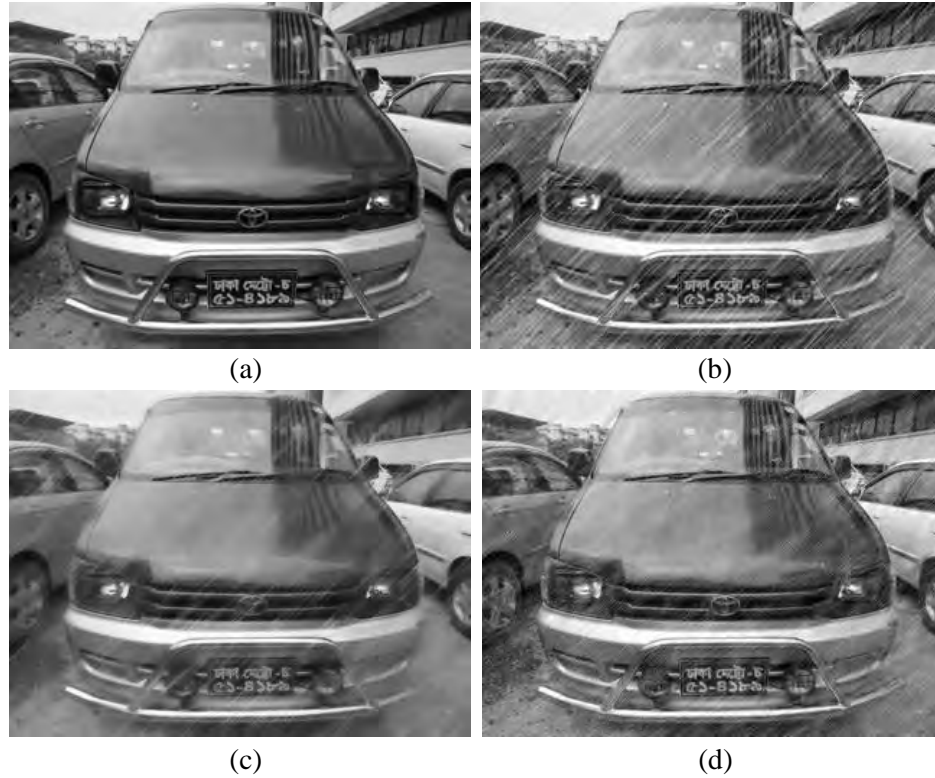


Figure 4.5: Example of (a) a simple non-rain car image, and it's (b) rain-affected version. (c) The rain-removed version after applying the technique [5] and (d) the rain-removed version after applying the proposed rain removal technique.

low frequency subbands. Then rain components are removed from the high frequency subbands by performing dictionary learning and sparse coding. But this approach takes much time compare to our rain removal technique. For the images of resolution  $320 \times 240$ , the average running time of technique [5] is 92.0 seconds, where our new rain removal technique takes only 0.27 seconds. That means the new approach is approximately 340 times faster than the technique [5]. Even the visual condition of the resulted image by the proposed technique is better than the existing technique [5]. Figure 4.5(a) shows a simple non-rain image and Figure 4.5(b) shows the same image after applying rain effects. Figure 4.5(c) is the result of the technique [5] which takes 95.50 seconds (with PSNR value 22.52 dB), and Figure 4.5(d) is the result of the proposed rain removal approach which takes only 0.26 seconds (with PSNR value 22.83 dB). Clearly, the proposed rain removal technique is better than the technique [5] in terms of running time, as well as, visual quality.



After removing rain effects from the image, we apply the proposed ALPD (with value of parameter  $k = 0.3$ ) on that 225 rain-removed car images. Figure 4.4 shows few examples of detected LP regions. Table 4.10 shows the status of the proposed ALPD for heavy, moderate and light rain-affected image sets. For each rain orientational image subsets (contains 15 images each), the ALPD gives one set of filtered LP areas. The detection rate (Equation 4.1) depends on the number of original LP areas that are put into the filtered LP set. From Table 4.10, the proposed ALPD have the average LP detection rate of 96.44% for rain-affected car images.

Table 4.10: Performance of the proposed ALPD on rain-affected car images (the rain removal technique is applied beforehand).

Level of rain effects	Rain orientation	No. of images	No. of original LPs	Detection rate (%)
Heavy	-45 deg	15	15	100
	-30 deg	15	15	100
	-15 deg	15	14	93.33
	0 deg	15	12	80
	+15 deg	15	15	100
	+30 deg	15	15	100
	+45 deg	15	15	100
Moderate	-45 deg	15	15	100
	-30 deg	15	15	100
	-15 deg	15	15	100
	0 deg	15	15	100
Light	-30 deg	15	14	93.33
	-15 deg	15	14	93.33
	+15 deg	15	14	93.33
	+30 deg	15	14	93.33

## 4.7 Experiment on Indoor, Day, Night, Blurry and Foggy Images

We tested the proposed ALPD on 300 non-rain car images from Bangla LP database [3]. These image set contains normal(day-light), fog affected, blurry, low contrast indoor and night images. Some example car images and detected LP regions by the proposed ALPD are shown in Figure 4.6. Table 4.11 shows the status of the proposed ALPD for

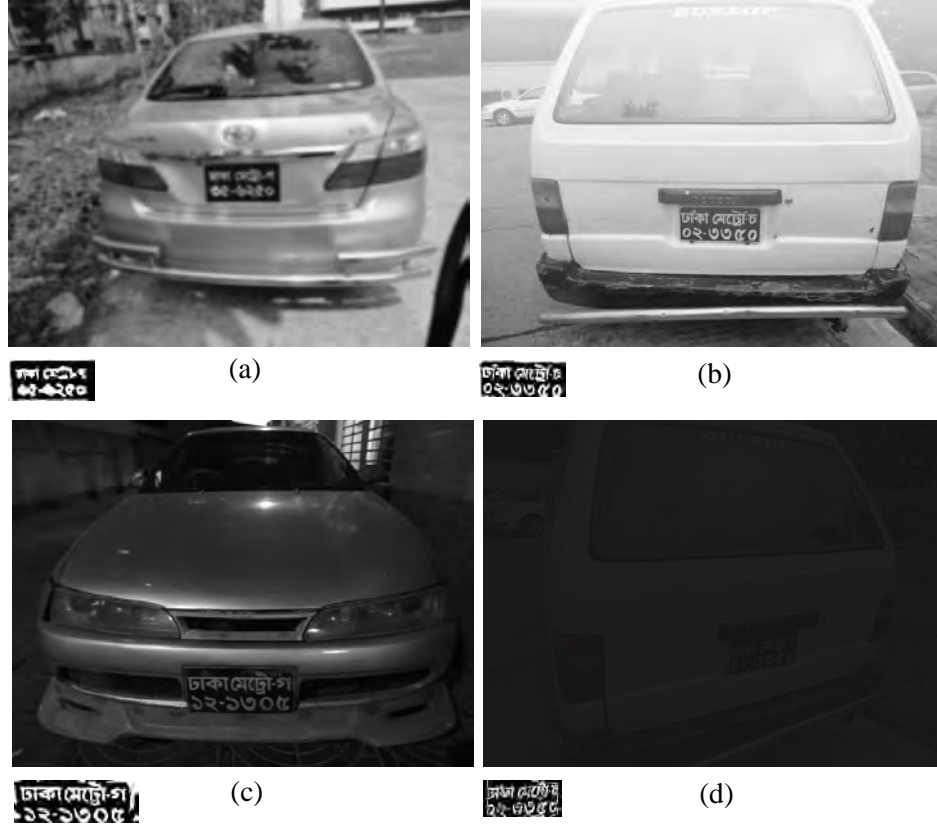


Figure 4.6: Example car images from Bangla LP database [3]. (a) Blur, (b) fog, (c) indoor and (d) night. Detected LP region (by the proposed ALPD) is given just below the individual image.

normal(day-light), fog affected, blurry, low contrast indoor and night image sets. During experiment, we have changed the value of parameter  $k$  to get the best output for different image conditions. Third column of the Table 4.11 shows the assigned values of parameter  $k$  for different image conditions. In this experiment, the average LP detection rate is 86.25%. In the Table, the proposed ALPD shows degraded performance (detection rate of 75%) for blurry images. This is due to lack of sharp edges between LP text and LP background. Although before filtering, the candidate LP regions (LP + non-LP) contains all the original LPs, but during filtering wrong selection causes performance degradation.

Table 4.11: Performance of the proposed ALPD on 300 non-rain car images having normal (day-light) and hazardous conditions (fog, blur, indoor and night).

Image condition	No. of images	Value of $k$	No. of original LPs	Detection rate (%)
Day-light	100	0.300	95	95.00
Fog	80	0.200	65	81.25
Blur	40	0.200	30	75.00
Indoor	40	0.300	39	97.50
Night	40	0.075	33	82.50

## 4.8 Performance of Horizontal Tilt Correction

In the proposed ALPD, we use a new approach for detection and correction of horizontally tilted LP. The new approach uses radon transform to detect tilt angle, and then apply necessary affine transformation and horizontal boundary elimination to make an LP correct. We test this approach on an image set of 125 detected [3] (but not tilt corrected) LP regions. These LP regions are automatically detected using the proposed ALPD (without using the proposed tilt correction approach). Figure 4.7 shows some example of detected LP regions without tilt correction. To make them correct, we apply the proposed radon transform-based tilt correction technique and find that almost 96% LP regions are become horizontally straight in orientation. Rest of them (4%) have negligible amount (1 or 2 degree) of orientation error. Figure 4.7 shows some example images of corrected LP region using the proposed tilt correction approach.

## 4.9 Comparison with Other Methods

We compare the proposed ALPD with two of the existing ALPD approaches [6] and [7]. We implement them into our machine using MATLAB 7.12 and applied on the English car image database [4] contains 325 images having different resolutions, various illumination conditions, and different types, tiltation and colors of LPs. Figure 4.8 shows some example car images from that image database. We also applied the proposed ALPD on this english car image database. The experimental results are summarized in Table 4.12. In the Table, the technique [6] shows poor performance (detection rate of 34.46%)

due to tilted LP, noise and low contrast image environment. No such special approach is taken in [6] to handle tiltation, low contrast, uneven illumination and noise problems. Moreover, the average running time is much higher than the proposed one, because method [6] uses large overlapping window of size 360 by 120 pixels to detect the vertical axis of symmetry. But in the proposed method, all types of overlapping spatial windows have the maximum size of 20 by 20 pixels. The technique [7] shows good performance (detection rate of 83.08%), but the average running time is much higher than the others due to applying time consuming order-static filter (Bernsen binarization) on the whole input image whereas, the proposed method uses Bernsen binarization method on a few small sized candidate LP regions. The detection rate of the proposed ALPD is outstanding (98.15%) and the average running time is only 0.45 seconds. In Figure 4.8, the detected LP regions by different ALPD methods are given for same input car image from [4].

In Section 4.4 and 4.5, we have tested the proposed ALPD on 525 car images (with or without hazardous conditions) having Bangla text LPs. Technique [6] and [7] are also applied on these car images to see their performance over hazardous conditions. Table 4.13 shows the summarized experimental results. Due to hazardous conditions, the technique [6] and [7] show degraded performance having only detection rate 12.20% and 45.14% respectively, whereas the proposed ALPD shows detection rate of 91.24%. In Figure 4.9, the detected LP regions by different ALPD methods are given for same input car image from [3].




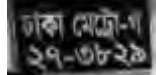

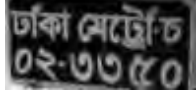

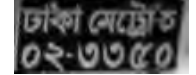


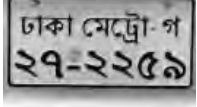
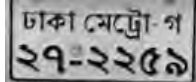

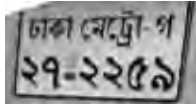
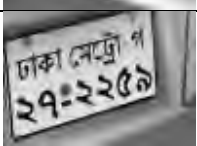
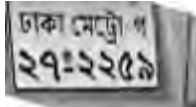

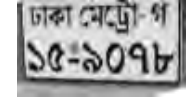

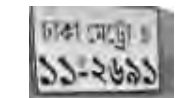
Detected LP regions using proposed ALPD (before tilt correction)	Automatically detected tilt angle	LP regions (after tilt correction)
	0 deg	
	10 deg	
	169 deg	
	10 deg	
	163 deg	
	179 deg	
	163 deg	
	17 deg	
	162 deg	
	19 deg	

Figure 4.7: Examples of detected LP image before tilt correction, as well as, after applying proposed Radon transform-based tilt correction. Automatically detected horizontal tilt angles are also given in the middle column of the Figure.










Car images having LP written in English	Detected LP regions	ALPD methods
		[6]
		[7]
		Proposed
	(Undetected due to tilted LP)	[6]
		[7]
		Proposed
	(Undetected due to low contrast night condition)	[6]
	(Undetected due to low contrast night condition)	[7]
		Proposed

Figure 4.8: Example car images from English LP database [4]. Here the top image has no hazardous condition, middle image has horizontally tilted LP and the bottom image has low contrast night condition. Also the detected LP regions by different ALPD methods are given.







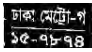

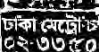
Car images having LP written in Bangla	Detected LP regions	ALPD methods
		[6]
		[7]
		Proposed
	(Undetected due to tilted LP)	[6]
		[7]
		Proposed
	(Undetected due to heavy rain streaks)	[6]
	(Undetected due to heavy rain streaks)	[7]
		Proposed

Figure 4.9: Example car images from Bangla LP database [3]. Here the top image has no hazardous conditions, middle image has horizontally tilted LP and the bottom image has rain effects. Also the detected LP regions by different ALPD methods are given.

Table 4.12: Performance of the ALPD techniques [6], [7] and the proposed one on English car image database [4].

ALPD methods	No. of detected LPs (out of 325 images)	Detection rate (%)	Average running time (seconds)
[6]	112	34.46	0.83
[7]	270	83.08	2.25
proposed	319	98.15	0.45

Table 4.13: Performance of the ALPD techniques [6], [7] and the proposed one on Bangla car image database [3].

ALPD methods	No. of detected LPs (out of 525 images)	Detection rate (%)	Average running time (seconds)
[6]	64	12.20	0.67
[7]	237	45.14	1.55
proposed	479	91.24	0.39

## 4.10 Conclusion

The proposed rain removal technique (used at the first stage of the proposed ALPD) is compared with an existing rain removal technique and shows better performance in terms of visual condition and running time. After removing rain streaks from 225 rain affected car images, the proposed ALPD is applied on them and find that the average LP detection rate is 96.44%. The performance of the proposed ALPD on non-rain 300 images having other hazardous (indoor, night, blurry and foggy) and normal (day-light) conditions is also well enough. It shows the average detection rate of 86.25%. Horizontal tilt correction ability of the proposed Radon transformed based approach is 96%. The results (detection rate and running time) obtained from the proposed ALPD method are compared with two of the existing ALPD methods [6, 7]. We compare the results for both Bangla and English LP database. All the experimental results prove that the proposed ALPD method performs significantly better than the two existing ALPD approaches.



## Chapter 5

# Conclusion

### 5.1 Summary

In this thesis, we present a new automatic license plate detection method consisting of five processing stages. In each stage, we develop new techniques and approaches capable of handling different hazardous conditions. In the first stage, we convert the input color image into a grayscale image and remove noises from the grayscale image. To handle rain (periodic noise) affected images, a novel rain removal technique is applied on the input grayscale image. The new rain removal technique removes rain streaks from image in an efficient way (image quality and running time). In the second stage, we introduce a new Tamura-CLAHE contrast enhancement approach for handling low contrast images (indoor, blur, fog, night) which enhances the contrast of the image in a reasonable way. After contrast enhancement, the proposed ALPD uses local irregularities (standard deviation) as a feature for LP localization, because LP areas have significant local irregularities due to plate character's density and background. To do this, a new statistical binarization method is used at the end of the second stage. In the third stage, local counting filter and morphological erosion-dilation is applied to preserve high dense white regions, fill holes and remove small thin white areas of the binary image. Then all the binary connected components are cropped from the input image and generates number of candidate LP regions. These candidate LP regions can be horizontally tilted due to camera position and angle. So in the fourth stage, a novel

Radon transform based LP tilt detection and correction method is applied on the candidate LP regions. In the candidate LP set, one is the original LP region and others are non-LPs. In the last stage, we filter-out most of the non-LP regions from the candidate LP set based on basic LP features such as, LP's size, ratio and orientation. Two new filtering approaches (entropy based and average counting based) are presented in this thesis for removing rest of the non-LPs. The proposed ALPD is implemented and tested on 850 car images having different hazardous conditions such as night, indoor, day, blur, foggy, rainy and tilted. The overall detection rate for these inputs is 94%. We also compare the experimental results against ALPD methods that were presented in the literature. We find that our proposed ALPD outperforms existing ALPD methods in terms of detection rate and running time.

## 5.2 Suggestions for Future Work

In the second stage of the proposed ALPD, we use a statistical binarization method where the parameter  $k$  depends on different image conditions (fog, rain, day, night, blur, indoor). The proposed ALPD uses static values of  $k$  for different types of images which are determined experimentally. However, the value of  $k$  can be determined dynamically based on amount of contrast, brightness and illumination condition of the image. In the proposed ALPD, the rain removal approach is applied only on the rain affected car images. There is no such steps to determine which input image is rain affected and which one is not. Image classification for rain and non-rain image can be employed for triggering the rain removal function. In future work, we intend to improve our ALPD to solve these problems. In addition, the proposed ALPD method can be improved by introducing more filtering criteria. We can associate more issues like snowy weather condition, vertically tilted LP to make the ALPD method robust. In order to apply our proposed scheme in real-time applications more efficiently, algorithms can be implemented in hard-wire and parallel devices, which require a lot of research in these fields.

# Bibliography

- [1] “USC-SIPI Image Database.” <http://sipi.usc.edu/database/>. [Online; accessed 24-July-2014].
- [2] R. Gonzalez and R. Woods, *Digital image processing, 3rd Edition*. Pearson, Prentice Hall, 2008.
- [3] “ALPD Image Database.”  
<https://sites.google.com/site/samicsemist/about-the-teacher/mscthesisdetails>.  
[Online; accessed 12-July-2014].
- [4] “English LP Database.”  
[http://www.zemris.fer.hr/projects/LicensePlates/english/baza\\_slika.zip](http://www.zemris.fer.hr/projects/LicensePlates/english/baza_slika.zip). [Online; accessed 12-July-2014].
- [5] L. W. Kang, C. W. Lin, and Y. H. Fu, “Automatic single-image-based rain streaks removal via image decomposition,” *IEEE Transactions on Image Processing*, vol. 21, no. 4, pp. 1742–1755, 2012.
- [6] M. Hasan, M. Ali, and M. Kabir, “Real time detection and recognition of license plate in bengali,” *A Technical Report submitted to University of California, Riverside, Bourns College of Engineering*, 2013.
- [7] Y. Wen, Y. Lu, J. Yan, Z. Zhou, K. Deneen, and P. Shi, “An algorithm for license plate recognition applied to intelligent transportation system,” *IEEE Transactions on Intelligent Transportation Systems*, vol. 12, no. 3, pp. 830–845, 2011.

- [8] “Automatic number plate recognition.”  
[http://en.wikipedia.org/wiki/Automatic\\_number\\_plate\\_recognition](http://en.wikipedia.org/wiki/Automatic_number_plate_recognition). [Online; accessed 20-May-2014].
- [9] S. Du, M. Ibrahim, M. Shehata, and W. Badawy, “Automatic license plate recognition(alpr): a state-of-the-art review,” *IEEE Transactions on Circuits and Systems for Video Technology*, vol. 23, no. 2, pp. 311–325, 2013.
- [10] C. Anagnostopoulos, I. Anagnostopoulos, I. Psoroulas, V. Loumos, and E. Kayafas, “License plate recognition from still images and video sequences: a survey,” *IEEE Transactions on Intelligent Transportation Systems*, vol. 9, no. 3, pp. 377–391, 2008.
- [11] Y. Wang, W. Lin, and S. Horng, “A sliding window technique for efficient license plate localization based on discrete wavelet transform,” *Elsevier Science, Expert systems with Applications*, vol. 38, no. 4, pp. 3142–3146, 2011.
- [12] A. Ghosh, S. Sharma, M. Islam, S. Biswas, and S. Akter, “Automatic license plate recognition (alpr) for bangladeshi vehicles,” *Global Journal of Computer Science and Technology, Global Journal Incorporation*, vol. 11, no. 21, pp. 69–73, 2011.
- [13] M. Joarder, K. Mahmud, T. Ahmed, M. Kawser, and B. Ahamed, “Bangla automatic number plate recognition system using artificial neural network,” *Asian Transactions on Science and Technology*, vol. 2, no. 1, pp. 1–10, 2012.
- [14] G. Hsu, J. Chen, and Y. Chung, “Application-oriented license plate recognition,” *IEEE Transactions on Vehicular Technology*, vol. 62, no. 2, pp. 552–561, 2013.
- [15] “Grayscale.” <http://en.wikipedia.org/wiki/Grayscale>. [Online; accessed 22-May-2014].
- [16] R. Gonzalez, R. Woods, and S. L. Eddins, *Digital image processing using Matlab, 2nd Edition*. Gatesmark Publisher, 2009.
- [17] A. K. Jain, *Fundamentals of Digital Image Processing, 1st Edition*. Pearson, Singapore, 2003.

- [18] H. Tamura, S. Mori, and T. Yamawaki, "Textural features corresponding to visual perception," *IEEE Transactions on Systems, Man and Cybernetics*, vol. 8, no. 6, pp. 460–473, 1978.
- [19] J. Bernsen, "Dynamic thresholding of gray-level images," *In Proceedings of 8th International Conference on Pattern Recognition, Paris, France*, pp. 1251–1255, 1986.
- [20] L. Shapiro and G. Stockman, *Computer vision, 1st Edition*. Prentice Hall, Upper Saddle River, NJ, USA, 2002.
- [21] K. Zuiderveld, "Contrast limited adaptive histogram equalization," *Graphic Gems IV, Academic Press Professional, Inc. San Diego, CA, USA*, pp. 474–485, 1994.
- [22] M. Goyal, "Morphological image processing," *International Journal of Computer Science and Technology*, vol. 2, no. 4, pp. 161–165, 2011.
- [23] K. Jafari-Khouzani and H. Soltanian-Zadeh, "Radon transform orientation estimation for rotation invariant texture analysis," *IEEE Transactions on Pattern Analysis and Machine Intelligence*, vol. 27, no. 6, pp. 1004–1008, 2005.
- [24] J. S. Lim, *Two-Dimensional Signal and Image Processing*. Englewood Cliffs, NJ, Prentice Hall, 1990.
- [25] C. Anagnostopoulos, I. Anagnostopoulos, V. Loumos, and E. Kayafas, "A license plate recognition algorithm for intelligent transportation system applications," *IEEE Transactions on Intelligent Transportation Systems*, vol. 7, no. 3, pp. 377–392, 2006.
- [26] Y. Huang, C. Chen, Y. Chang, and F. Sandnes, "An intelligent strategy for checking the annual inspection status of motorcycles based on license plate recognition," *Elsevier Science, Expert Systems with Applications*, vol. 36, no. 5, pp. 9260–9267, 2009.
- [27] K. Deb, H. Chae, and K.H.Jo, "Vehicle license plate detection method based on sliding concentric windows and histogram," *Journal of Computers*, vol. 4, no. 8, pp. 771–777, 2009.

- 
- [28] M. Bertozzi, A. Broggi, A. Fascioli, and S. Nichele, “Stereo vision-based vehicle detection,” *In Proceedings of IEEE Intelligent Vehicles Symposium, Dearbon (MI), USA*, pp. 39–44, 2000.